OPTOMECHANICAL QUANTUM MEMORY FOR PHOTON STORAGE

David Cirauqui Garcia

Supervisor: Anders Søndberg Sørensen

Co-supervisor: Luca Dellantonio

KØBENHAVNS UNIVERSITET

Theoretical Quantum Optics

Niels Bohr Institutet

Københavns Universitet

Denmark

September, 2018

Abstract

Efficient, ultra-fast photon storage is one of the basic requirements for building a quantum computer and process quantum information. Several schemes for a quantum memory have been proposed, but none based on optomechanical systems. These systems are known to have very long coherence times, and thus are a promising architecture. In this thesis, we consider an optical cavity with an optomechanical membrane as a mirror, and study how a single photon couples to the vibrational motion. We control this storage process by means of a coherent light field, which we optimise in the adiabatic regime. We explore the non adiabatic regime numerically and develop a mathematical framework that allows us to study it analytically. Our mathematical method is not restricted to an optomechanical cavity, and can easily be extended to other physical systems. With the analytical results derived, we can give a recipe for a better optimisation of the non adiabatic storage of photons. In particular, we find a class of single photon shapes that performs better than all others, with which the adiabatic condition is fulfilled for shorter timescales.

Acknowledgements

I would like to thank my supervisor Anders Søndberg Sørensen, for sharing his knowledge, coming up with interesting ideas for my thesis, and for helping me throughout all this work. I am grateful and honoured to have been able to work with him.

My acknowledgements to Luca Dellantonio truly deserve a section. Not only he convinced me to join the theoretical quantum optics group, but he also co-supervised this work. He managed to keep me motivated when I needed the most. This thesis would not have been what it is today without his feedbacks and wise advices. My special and most sincere thanks to him.

Finally, I thank my closest ones: those who know how tough this last year has been for me, and still have been there on the phone every single time I needed it. It is said that life is a rollercoaster, and lately I have needed their help to climb it, more times than I would have liked. Thank you all.

Per últim, m'agradaria fer menció a tots aquells que, sabent com de difícil ha sigut aquest últim any per a mi, han tingut paciència i han sigut a l'altra banda del telèfon cada vegada que ho he necessitat. És dit que la vida és un seguit d'altibaixos, i últimament he necessitat la seva mà per poder escalar moltes més vegades de les que idealment m'hagués agradat. Us estic profundament agraït, i us envio una forta abraçada allà on sigui que estigueu.

A tots els nens de dotze anys que somien en ser físics. A tots aquells que els recolzen i els ajuden a fer realitat el seu somni. A tots els nens de vint-i-quatre anys que no han deixat mai de somiar.

Sóc físic, per fi.

Contents

List of Figures

Chapter 1

Introduction

Physics is dead

-"There is nothing new to be discovered in physics now. All that remains is more and more precise measurement."- Lord Kelvin

-"It seems probable that most of the grand underlying principles have been firmly established. An eminent physicist remarked that the future truths of physical science are to be looked for in the sixth place of decimals."- Albert Michelson

These two sentences pronounced by Kelvin and Michelson at late 19th century are, probably, among the most famous in history of science. Yet the most unfortunate ones. By that time, thermodynamics and electromagnetism had just been introduced and were expected soon to be fully explored. Theoretical physics was dead, and it was time for experimentalists and engineers to rise and to take control of science.

More than ever before

-"This spooky action at a distance."- Albert Einstein

-"I think I can safely say that nobody understands quantum mechanics."- Richard Feynman

Only few years later, Planck explained Black Body Radiation and founded quantum mechanics. Few years later Einstein used the same theory to explain the photoelectric effect. These two long-lasting problems, that had given many troubles during past decades,

proved that there was a whole new theory to be developed. Quantum physics was officially born, and more new possibilities, properties, answers and questions than ever before were brought into the game.

During the last century, quantum theories have been further developed, and shown many interesting phenomena that cannot be described within a classical framework. Nowadays, there is no doubt: quantum mechanics is the future. From quantum computing and teleportation to material science and nanoscale engineering, the quantum world offers us unimaginable possibilities, yet to be explored and understood.

1.1 Quantum computers

In particular, two of the most *spooky* properties of quantum mechanics, namely entanglement and state superposition, have shown to exponentially speed up the computing capacity, both in theory [20][21] and in experiment [22][23]. The quantum equivalent of classical bits, (either 0 or 1), are *qubits*, which can be in a superposition of these two states, $|\psi\rangle = \alpha\,|0\rangle + \beta\,|1\rangle$ with $\|\alpha\|^2 + \|\beta\|^2 = 1$. Fast parallel information processing is thus included in the fundamental brick of a quantum computer. Photons are usually chosen for carrying quantum states through optical fibers and nanophotonic structures, since they weakly interact with the environment and have long coherence times [14]. Light-matter interaction is thus a prime field of study nowadays.

We refer to a *quantum computer* as an experimental set-up that is able to exploit these (and others) quantum mechanical properties to efficiently carry on computations and information processing over quantum states. In order to do so, a quantum computer must satisfy the di Vincenzo criteria [1]:

1. Scalability: several qubits are needed to work together to run complex problems.
2. Initialisation: qubits need to be initialised into a known state.
3. Universal gate operations: it must be possible to perform single and 2-qubit gate operations with a high fidelity.
4. Readout: qubits must be available for measurement.
5. Deoherence: qubits must have a coherence time much larger than the operation time.
6. Quantum interfaces for qubit interconversion: qubit interfaces must be possible for storage and on-chip communication between qubit registers.

7. Quantum interfaces to flying qubits for optical communication: qubit-photon interfaces must be available for long-distance transfer of quantum states and entanglement.

Conditions 1-5 are needed for quantum computation tasks, whereas conditions 6 and 7 are required for quantum communications.

There mainly exist two different approaches to the experimental implementation of quantum computers: trapped ions and superconducting qubits. Ion traps have large coherence times: most of current experiments achieve timescales larger than miliseconds [2] (about two orders of magnitude above the time needed for carrying on a quantum computation), while some groups demonstrate seconds [24] and even minutes [25]. However, trapped ion quantum computers have traditionally had a very difficult scalability, even though a lot of promising research in this direction is currently going on [14]. On the other hand, superconducting circuits are more easily scalable, with experiments demonstrating systems of up to 7 [15] and even 9 qubits [18][19], but noise from the environment usually lead to bad coherence times [3]. All other diVincenzo conditions for quantum computation (2,3,4) are possible to achieve for both families of quantum computers.

Most promising (in a short term) architectures for universal quantum computers include, therefore, hybrid platforms with components based on different experimental approaches.

1.2 Quantum memories

Lastly, in order to perform quantum communications, a quantum computer must be able to store and transfer quantum states along long distances. This can be mostly achieved by a system which is capable to store and retrieve photons on demand, ensuring that its information is not altered in such process, by a strong coupling between different elementary excitations such as photons, phonons or spin waves.

In this thesis, we focus on the study of quantum memories for the efficient storage of photons, in particular to an optomechanical scheme. Optomechanical membranes can be cooled down to its ground state, thus achieving single phonon control [13] [16]. They can also be engineered to have resonant frequencies in the GHz range and a strong coupling between the light field and the mechanical motion. Therefore, they provide a promising scheme for storage and retrieval of ultra short light pulses [17], allowing to achieve single photon-single phonon state swap, which ensures a high-fidelity information transfer.

1.3 Objectives and outline

The main objective of this thesis is the study and optimisation of an optomechanical quantum memory for the storage of photons. The outline of this thesis is as follows.

- **Chapter 1. Introduction.** Introduces the reader to the field of study, objectives and motivation of this thesis.
- **Chatper 2. Theoretical basics of optomechanics.** Introduces necessary concepts of optomechanical quantum optics and presents the derivation of the basic equations used in following chapters.
- **Chapter 3. First approach: the dirty experiment.** Presents a first approach to the study of the dynamics of a membrane in an optomechanical quantum memory scheme.
- **Chapter 4. An optomechanical quantum memory.** First, the adiabatic regime of an optomechanical quantum memory is studied and optimised. Later, a numerical exploration of the non adiabatic regime is carried on, and a mathematical framework is developed to study it analytically. By means of this framework, several features are identified and a recipe for an improved storage strategy is provided.
- **Chapter 5. Conclusions and outlook.** The results of the thesis are summarised, and an outlook for further researches and potential improvements is given.

Chapter 2

Theoretical basics of optomechanics

The main goal of this work is to study an optomechanical quantum memory for photon storage. In this chapter we present a compact optomechanical review for understanding the thesis. In order to describe the system we are interested in, we study optical fields inside a cavity (cavity optics), starting with the simplest possible case and adding to it, step by step, more complex, interesting and realistic features. The equations derived in this chapter will later be used in following ones, and will constitute the basis of this work.

In this order, we consider these systems:

1. A perfect cavity with completely reflective mirrors, from both a classical and a quantum point of view.

2. A lossy cavity, in which one of the mirrors is not perfect, but partially transparent, thus allowing the outside field to leak in and the inside field to leak out.

3. Finally, we attach only one of the mirrors to a spring in order to include the mechanical degree of freedom of the desired optomechanical system. The work done in the following chapters of this thesis is based on this last system.

2.1 Perfect cavity

Consider an optical cavity along the z-axis with perfectly reflective mirrors that keep the light inside the cavity. For simplicity, assume that we have a single-mode electromagnetic field inside it. In order to satisfy Maxwell's equations and the boundary conditions imposed by the mirrors, such field must form standing waves that are described by the equations:

$$E_x = E_0 q\left(t\right) sin\left(kz\right), \tag{2.1}$$

$$B_y = B_0 p\left(t\right) cos\left(kz\right), \tag{2.2}$$

with $E_0 = \left(\frac{2\omega^2}{\epsilon_0 V}\right)^{\frac{1}{2}}$ and $B_0 = \frac{\mu_0 \epsilon_0}{k}\left(\frac{2\omega^2}{\epsilon_0 V}\right)^{\frac{1}{2}}$. Here, V is the cavity volume, ω the frequency of the mode inside the cavity, and $k = \frac{\omega}{c}$ the wave number ($c = \frac{1}{\sqrt{\epsilon_0 \mu_0}}$ is the speed of light in vacuum, and ϵ_0 and μ_0 the vacuum electric permitivity and magnetic permeability). We also assume, for sake of simplicity, that the electric field is polarised along the x-axis and the magnetic field is polarised along the y-axis. All time dependence is encoded in the functions $q\left(t\right)$ and $p\left(t\right)$, which represent canonical position and momentum, respectively ($p\left(t\right) = \dot{q}\left(t\right)$).

The total energy (or the Hamiltonian of the system) of the electromagnetic field inside a volume V is given by:

$$H = \frac{1}{2}\int_V \left[\epsilon_0 \|E\|^2 + \frac{1}{\mu_0}\|B\|^2\right] dV. \tag{2.3}$$

By writing this expression and substituting the electromagnetic field in a perfect cavity, eq.2.1-2.2, we get:

$$H = \frac{1}{2}\left[\omega^2 q^2\left(t\right) + p^2\left(t\right)\right]. \tag{2.4}$$

Noticeably, this is equal to the total energy of a harmonic oscillator with an effective unitary mass and a frequency ω.

2.1.1 Quantisation of the electromagnetic field

Above we described an electromagnetic field inside a perfect cavity from a classical point of view, eq.2.4. In order to quantise it, we need to generalise the canonical position and momentum to operators. The Hamiltonian operator of the system is thus:

$$\hat{H} = \frac{1}{2}\left[\omega^2 \hat{q}^2\left(t\right) + \hat{p}^2\left(t\right)\right], \tag{2.5}$$

where the operators $\hat{p}\left(t\right)$ and $\hat{q}\left(t\right)$ have canonical commutation relation $\left[\hat{q}\left(t\right), \hat{p}\left(t'\right)\right] = i\hbar\delta\left(t - t'\right)$.

We introduce the creation and annihilation operators (or ladder operators) for the light field:

$$\hat{a} = \frac{1}{\sqrt{2\hbar\omega}}\left(\omega\hat{q} + i\hat{p}\right), \tag{2.6}$$

$$\hat{a}^\dagger = \frac{1}{\sqrt{2\hbar\omega}}\left(\omega\hat{q} - i\hat{p}\right), \tag{2.7}$$

that act on a photonic number state $|n\rangle$ according to

$$\hat{a}\left|n\right\rangle = \sqrt{n}\left|n-1\right\rangle, \tag{2.8}$$

$$\hat{a}^\dagger |n\rangle = \sqrt{n+1}\,|n+1\rangle\,. \tag{2.9}$$

From the commutation relation between $\hat{p}(t)$ and $\hat{q}(t)$ and the definitions eq.2.6 and eq.2.7 it is possible to prove that

$$\left[\hat{a}(t), \hat{a}^\dagger\left(t'\right)\right] = \delta\left(t - t'\right). \tag{2.10}$$

The Hamiltonian of our system can be rewritten in terms of the ladder operators $\hat{a}$ and $\hat{a}^\dagger$:

$$\hat{H} = \hbar\omega\left(\hat{n} + \frac{1}{2}\right), \tag{2.11}$$

where we introduced the number operator $\hat{n}$, with the number states as its eigenstates:

$$\hat{n} = \hat{a}^\dagger\hat{a} \tag{2.12}$$

$$\hat{n}\,|n\rangle = n\,|n\rangle \tag{2.13}$$

Eq.2.13 can be proven from eq.2.8 and eq.2.9, and the definition eq.2.12. These number states are, therefore, the eigenstates of the Hamiltonian, $\hat{H}\,|n\rangle = E_n\,|n\rangle$, with eigenenergies $E_n = \hbar\omega\left(n + \frac{1}{2}\right)$. The quantised electromagnetic fields $\hat{E}$ and $\hat{B}$ can thus be rewritten as

$$\hat{E} = E_q\left(\hat{a} + \hat{a}^\dagger\right) sin\,(kz)\,, \tag{2.14}$$

$$\hat{B} = B_q\left(\hat{a} - \hat{a}^\dagger\right) cos\,(kz)\,, \tag{2.15}$$

where $E_q = \left(\frac{\hbar\omega}{\epsilon_0 V}\right)^{\frac{1}{2}}$ and $B_q = -i\frac{\mu_0}{k}\left(\frac{\epsilon_0\hbar\omega^3}{V}\right)^{\frac{1}{2}}$.

The time evolution of the electromagnetic field and, in general, of any operator $\hat{O}$, is given by the Heisenberg equation:

$$\frac{d\hat{O}}{dt} = \frac{i}{\hbar}\left[\hat{H}, \hat{O}\right] + \frac{\partial\hat{O}}{\partial t}. \tag{2.16}$$

2.2 Lossy cavity

Above we considered a perfectly reflecting cavity, treated as an independent system completely isolated from the outside world. A more realistic scenario is the one where the mirrors are partially transparent, so that the field inside the cavity can interact with an incoming light field (see fig.2.1). It is very useful to treat this system with a beamsplitter model.

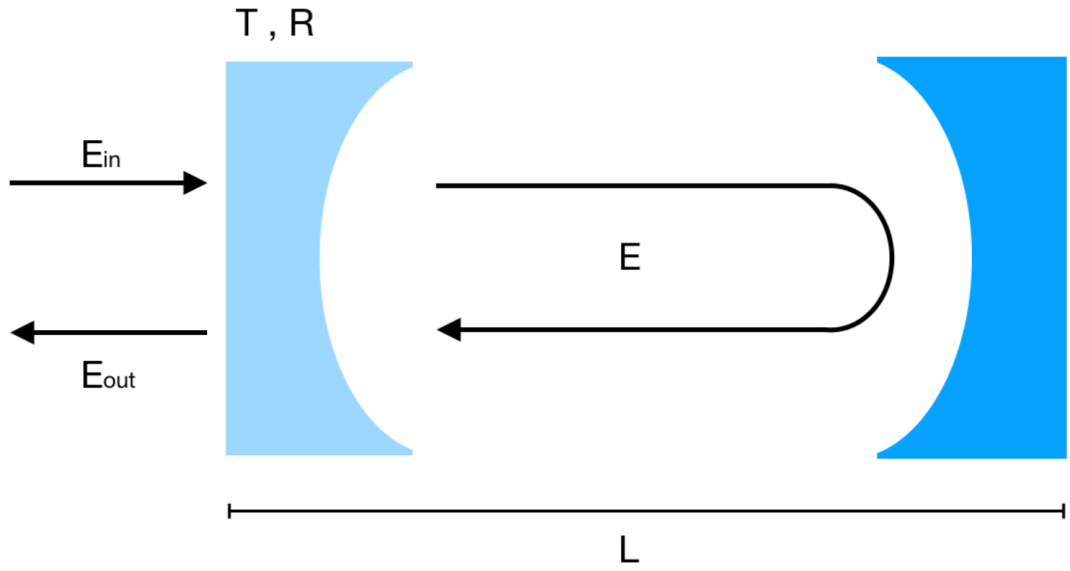

Figure 2.1: Scheme of a cavity with a partially transparent mirror. E is the electric field inside the cavity, E_{in} is the incident electric field and E_{out} is the output field. T and R are the transmission and reflection coefficients, respectively.

2.2.1 Classical model

From a classical point of view, an incoming field E_{in} sent towards a partially reflecting mirror has a probability T to enter the cavity and R to be reflected, where T and R are the reflecting and transmitting coefficients, respectively. Therefore, the electric field inside the cavity is described by the relation:

$$E\left(t+\Delta t\right)=TE_{in}+RE\left(t\right), \tag{2.17}$$

where $\Delta t=\frac{2L}{c}$ is the time of a roundtrip. In the limit $\Delta t\rightarrow 0$, we can use this last equation eq.2.17 to find the time derivative of the electric field $E\left(t\right)$, and thus its equation of motion:

$$\frac{dE}{dt}=\left(R-1\right)\frac{c}{L}E\left(t\right)+T\frac{c}{L}E_{in}\left(t\right). \tag{2.18}$$

The cavity loss rate κ is defined as the inverse of the lifetime of the electric field in the cavity, and can be found to be:

$$\frac{\kappa}{2}=\left(1-R\right)\frac{c}{L}. \tag{2.19}$$

If we assume our mirror to be perfect, in the sense that it does not absorb any energy, $R^2+T^2=1$ and κ can be approximated, in the limit of high reflectivity, $T\ll 1$, to:

$$\kappa\approx T^2\frac{c}{L}. \tag{2.20}$$

In terms of the cavity loss rate, the equation describing the classical evolution of the field inside the cavity becomes:

$$\frac{dE\left(t\right)}{dt}=-\frac{\kappa}{2}E\left(t\right)+\sqrt{\kappa}\left(\frac{L}{c}\right)^{\frac{1}{2}}E_{in}\left(t\right). \tag{2.21}$$

To compute the field outside the cavity, we use the input-output relation that:

$$E_{out}\left(t\right)=\left(\kappa\frac{L}{2c}-1\right)E_{in}\left(t\right)+\sqrt{\kappa}\left(\frac{L}{c}\right)^{\frac{1}{2}}E\left(t\right), \tag{2.22}$$

which, together with eq.2.21, gives a full description of the time evolution of the electric field in our system.

2.2.2 Quantum model

As we did before in setion 2.1, we quantise the electric field by replacing the classical variable $E\left(t\right)$ with the creation (anihilation) operator $\hat{a}\left(t\right)$ ($\hat{a}^{\dagger}\left(t\right)$). In order to quantise eq.2.21 we introduce the operator $\hat{\mathcal{F}}$: the quantum noise (and eventually drives) associated with the external vacuum field leaking in. The equation of motion, eq.2.21 becomes:

$$\dot{\hat{a}}=-\frac{\kappa}{2}\hat{a}+\hat{\mathcal{F}}. \tag{2.23}$$

To find the form of $\hat{\mathcal{F}}$, we assume that the cavity field $\hat{a}$ interacts with a continuum of modes, at different frequencies ω_k. The action of this reservoir is modeled by the operator $\hat{R}$:

$$\hat{R}^{\dagger}=-i\hbar\sum_{k}c_k\hat{a}_k^{\dagger}e^{\omega_k t} \tag{2.24}$$

Where the coefficients c_k define the coupling strengths between the modes k and the field inside the cavity. The transmission properties of the mirrors completely determine all the parameters c_k. The interaction Hamiltonian can then be found as $\hat{H}_I=-\hat{R}^{\dagger}\hat{S}-\hat{S}^{\dagger}\hat{R}$ (where $\hat{S}=\hat{a}$ is the operator describing the system and $\hat{R}$ the reservoir), which yields:

$$\hat{H}_I=i\hbar\sum_{k}c_k\hat{a}\hat{a}_k^{\dagger}e^{-i(\omega-\omega_k)t}+h.c. \tag{2.25}$$

We moved to a frame rotating at the cavity field's frequency ω.

Using the interaction Hamiltonian, eq.2.25 we can obtain the equations of motion for both the field inside the cavity and the reservoir modes:

$$\dot{\hat{a}}=-\sum_{k}c_k^{*}\hat{a}_k e^{i(\omega-\omega_k)t}, \tag{2.26}$$

$$\dot{\hat{a}}_k = c_k \hat{a} e^{-i(\omega-\omega_k)t}. \tag{2.27}$$

By formally integrating eq.2.27, the time evolution of the reservoir modes $\hat{a}_k$ is found to be:

$$\hat{a}_k(t) = \hat{a}_k(0) + \int_0^t dt' c_k \hat{a}(t') e^{-i(\omega-\omega_k)t'}, \tag{2.28}$$

that can be plugged into eq.2.26 to derive the equation of motion for the field inside the cavity, $\hat{a}$:

$$\dot{\hat{a}}(t) = -\sum_k c_k^* e^{i(\omega-\omega_k)t} \hat{a}_k(0) - \sum_k \|c_k\|^2 \int_0^t dt' \hat{a}(t') e^{i(\omega-\omega_k)(t-t')}. \tag{2.29}$$

Imposing the Wigner-Weisskopf approximation in the integral in eq.2.29, we can treat the oscillating term as a delta function. Thus, comparing with eq.2.23, we get:

$$\kappa = 2\pi \sum_k \|c_k\|^2 \delta(\omega - \omega_k) = 2\pi \|c_k\|^2 D(\nu) \tag{2.30}$$

where $D(\nu)$ is the density of states. Also, we can formally define the noise operator as:

$$\hat{\mathcal{F}} = -\sum_k c_k^* e^{i(\omega-\omega_k)t} \hat{a}_k(0). \tag{2.31}$$

With this derivation (so called microscopic noise model [4]), we see how the partially transmitting mirror allows the cavity to interact with the external world: the inside field can leak out at rate $\frac{\kappa}{2}$, and the continuum of modes can leak in the from of a drive and/or a noise term. Importantly, for the canonical commutation relation $\left[\hat{a}(t), \hat{a}^\dagger(t')\right] = \delta(t-t')$ to hold, quantum mechanics needs this noise term to exist (one can indeed check that, setting $\hat{\mathcal{F}} = 0$, eq.2.23 leads to a violation of the commutation relation).

As we did in the classical case, to have a full description of the dynamics of the light field we derive an input-output relation in the quantum regime. Identifying the noise at time $t = 0$ term as the input field

$$\hat{\mathcal{F}}_{in}(t) = -\sum_k c_k^* \hat{a}_k(0) e^{i(\omega-\omega_k)t}, \tag{2.32}$$

it makes sense to define the output field as the same term, but at any desired time t

$$\hat{\mathcal{F}}_{out}(t) = -\sum_k c_k^* \hat{a}_k(t) e^{i(\omega-\omega_k)t}. \tag{2.33}$$

Plugging eq.2.33 in the solution for the reservoir modes $\hat{a}_k(t)$ found above eq.2.28, yields:

$$\hat{\mathcal{F}}_{out}(t) = -\sum_k c_k^* \hat{a}_k(0) e^{i(\omega-\omega_k)t} - \sum_k \|c_k\|^2 \int_0^t dt' \hat{a}(t') e^{i(\omega-\omega_k)(t-t')}. \tag{2.34}$$

Identifying the first term as the input field, and recalling the definition of κ, eq.2.30, we finally get:

$$\hat{\mathcal{F}}_{out}(t) = \hat{\mathcal{F}}(t) - \kappa \hat{a}(t), \tag{2.35}$$

that is valid in the Wigner-Weisskopf approximation

Finally, we define the input and output fields:

$$\hat{a}_{in,out} = \frac{\hat{\mathcal{F}}_{in,out}}{\sqrt{\kappa}}, \tag{2.36}$$

to have them fulfilling the desired commutation relation eq.2.10. Plugging these definitions in the previous equations, we derive the fundamental equations describing the light field in a lossy cavity:

$$\dot{\hat{a}} = -\frac{\kappa}{2}\hat{a} + \sqrt{\kappa}\hat{a}_{in} \tag{2.37}$$

$$\hat{a}_{out} = \hat{a}_{in} - \sqrt{\kappa}\hat{a} \tag{2.38}$$

2.2.3 Strong coherent field as input

So far we described the input field as a quantum operator. Nevertheless, in many cases it is practical to include, in addition to the quantum field, a coherent field described by a classical function. In this new scenario, the interaction Hamiltonian is:

$$\hat{H}_I' = \hat{H}_I + i\hbar\sqrt{\kappa}\left[s_{in}(t)\,\hat{a}^\dagger - s_{in}^*(t)\,\hat{a}\right], \tag{2.39}$$

where $\hat{H}_I$ is defined in eq.2.25 and the classical light field is:

$$s_{in}(t) = \bar{s}_{in}e^{i\omega_L t}. \tag{2.40}$$

Here, ω_L is the frequency of the laser, and $\bar{s}_{in}$ its amplitude. In a rotating frame at this frequency, ω_L, the full Hamiltonian reads:

$$\hat{H} = -\hbar\Delta\hat{a}^\dagger\hat{a} + \hat{H}_I + i\hbar\sqrt{\kappa}\left[\bar{s}_{in}\hat{a}^\dagger - \bar{s}_{in}^*\hat{a}\right], \tag{2.41}$$

from which the equation of motion of the field inside the cavity can be derived to be:

$$\dot{\hat{a}} = -\left(i\Delta + \frac{\kappa}{2}\right)\hat{a} + \sqrt{\kappa}\left(\bar{s}_{in} + \hat{a}_{in}\right). \tag{2.42}$$

The parameter $\Delta = \omega - \omega_L$ is the detuning between the incoming classical field and the resonant frequency of the cavity.

Equation 2.42 generalises eq.2.37 to the case in which the input field is the sum of a strong coherent field s_{in} and a quantum noise $\hat{a}_{in}$. In this framework, we can also linearise

the field inside the cavity. The large, classical incoming field creates another large, classical field inside the cavity, and the incoming quantum fluctuations create a quantum field. Their equations of motion can be decoupled:

$$\bar{a} = \frac{\sqrt{\kappa}}{i\Delta + \frac{\kappa}{2}} \bar{s}_{in}, \tag{2.43}$$

$$\delta\dot{\hat{a}} = -\left(i\Delta + \frac{\kappa}{2}\right)\delta\hat{a} + \sqrt{\kappa}\hat{a}_{in}, \tag{2.44}$$

where $\hat{a} = \bar{a} + \delta\hat{a}$. Analogously, the input-output relations can be generalised:

$$\hat{a}_{out} = \hat{a}_{in} - \sqrt{\kappa}\hat{a}, \tag{2.45}$$

$$s_{out} = s_{in} - \sqrt{\kappa}\bar{a}. \tag{2.46}$$

This completes the quantum description of a cavity with a partially transparent mirror and an input consisting of a large, classical state plus a quantum field.

2.3 Adding an optomechanical membrane

Consider now the system described in previous sections, and let the perfectly reflecting mirror to move. The momentum carried by the light inside the cavity can thus be transformed into mechanical motion (vibration of the membrane). Such a system can be physically modeled by letting the membrane's mirror be attached to a spring, such that it has a mechanical degree of freedom, see fig.2.2.

The spring is described by a harmonic oscillator which Hamiltonian can be expressed, in terms of the position and momentum operators, as:

$$\hat{H}_M = \frac{m\Omega_m^2}{2}\hat{x}^2 + \frac{\hat{p}^2}{2m}. \tag{2.47}$$

Here, m is the mass of the membrane and Ω_m its resonant frequency. The operator $\hat{x}$ describes the position of the membrane with respect to its equilibrium.

The field inside the cavity interacts with the mechanical movement of the spring with a factor $G = \frac{\partial\omega}{\partial x}$, the so called optomechanical coupling. G is the first order variation in the characteristic frequency of the cavity and gives raise to the interaction:

$$\hat{H}_{IM} = \hbar G\hat{x}\hat{a}^\dagger\hat{a}. \tag{2.48}$$

It follows that the cavity experiences a frequency shift due to the change in its length, given by the coupling factor G and the membrane's position:

$$\dot{\hat{a}} = -\left[\frac{\kappa}{2} + i\left(\Delta - G\hat{x}\right)\right]\hat{a} + \hat{\mathcal{F}}_{in}. \tag{2.49}$$

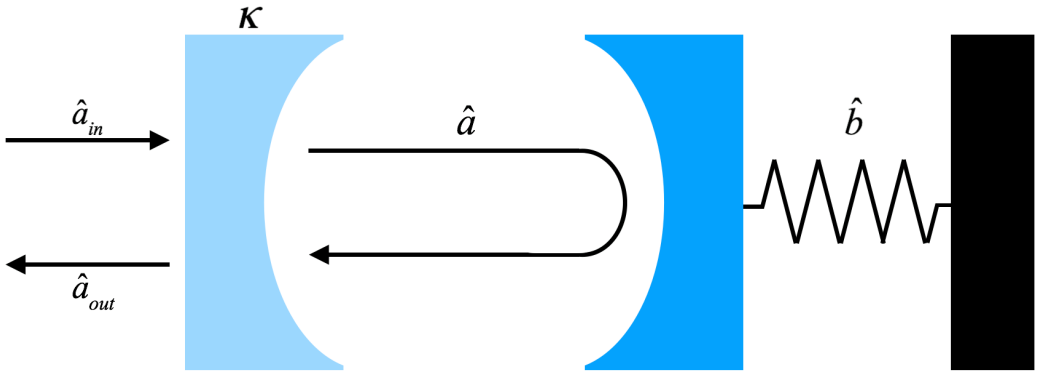

Figure 2.2: Scheme of an optomechanical cavity, where one of the mirrors is allowed to move in the transverse direction. Here, $\hat{a}$ is the field inside the cavity and $\hat{a}_{in/out}$ describe the input/output fields. κ is the cavity loss rate and $\hat{b}$ is the mechanical annihilation operator.

In eq.2.49, a vacuum input has been assumed, but this could be extended to any incoming field. Moreover, we can determine the force that the field inside the cavity exerts to the membrane. We define this radiation force as the variation of momentum that the membrane experiences due to the photon collisions, given by

$$\hat{F}_{RP} = \dot{\hat{p}} = -\hbar G \underbrace{\hat{a}^\dagger \hat{a}}_{\hat{n}} \tag{2.50}$$

The radiation pressure is directly proportional to the number of photons in the cavity, each of them transferring a momentum to the optomechanical membrane.

Now we extend the quantum description of the cavity, including the mechanical degree of freedom. In this work we are interested in the quantum mechanical description of the elementary vibrational motion of the membrane: the phonon. Phonons can be defined in a similar manner as we did for photons in eq.2.6 and eq.2.7.

Thus, as we did for the photon creation and annihilation operators, $\hat{a}^\dagger$ and $\hat{a}$, we introduce the mechanical ladder operators $\hat{b}^\dagger$ and $\hat{b}$. These act over phonon number quantum states, $|n_b\rangle$, in the same way as the photon operators act over $|n\rangle$, eq.2.8-2.9. In terms of $\hat{b}$ and $\hat{b}^\dagger$, the operators for the position and the momentum read, respectively:

$$\hat{x} = \left(\frac{\hbar}{2m\Omega_m}\right)^{\frac{1}{2}} \left(\hat{b} + \hat{b}^\dagger\right), \tag{2.51}$$

$$\hat{p} = i\left(\frac{\hbar m\Omega_m}{2}\right)^{\frac{1}{2}} \left(\hat{b} - \hat{b}^\dagger\right). \tag{2.52}$$

The standard commutation relation $\left[\hat{b}\left(t\right),\hat{b}^{\dagger}\left(t'\right)\right]=\delta\left(t-t'\right)$ holds.

If we rewrite the Hamiltonian in eq.2.47 in terms of $\hat{b}$ and $\hat{b}^{\dagger}$, we find it to be formally identical to the optical system Hamiltonian:

$$\hat{H}_M=\hbar\Omega_m\left(\underbrace{\hat{b}^{\dagger}\hat{b}}_{\hat{n}_b}+\frac{1}{2}\right) \tag{2.53}$$

Here we can also identify the number of phonons operator, $\hat{n}_b=\hat{b}^{\dagger}\hat{b}$. For the interaction Hamiltonian that couples the mechanical motion and the optical field, eq.2.48, we find:

$$\hat{H}_{IM}=\hbar G x_{zpf}\left(\hat{b}+\hat{b}^{\dagger}\right)\hat{a}^{\dagger}\hat{a}, \tag{2.54}$$

where $x_{zpf}=\sqrt{\langle 0|\,\hat{x}^2\,|0\rangle}=\left(\frac{\hbar}{2m\Omega_m}\right)^{\frac{1}{2}}$ is the zero point motion fluctuation of the operator $\hat{x}$.

As we did in previous sections for a cavity with a partially transparent mirror and no membrane, consider now that the input field is the sum of a large, classical field plus a small quantum fluctuation. Then, it is practical to linearise the field inside the cavity, separating the two contributions $\hat{a}=\bar{a}+\delta\hat{a}$. By doing so, the interaction Hamiltonian can be rewritten as:

$$\hat{H}_{IM}=\hbar g\underbrace{\left[\delta\hat{a}^{\dagger}\hat{b}^{\dagger}+\delta\hat{a}\hat{b}\right]}_{(1)}+\hbar g\underbrace{\left[\delta\hat{a}\hat{b}^{\dagger}+\delta\hat{a}^{\dagger}\hat{b}\right]}_{(2)} \tag{2.55}$$

where we defined the field-enhanced coupling rate $g=Gx_{zpf}\bar{a}$. From eq.2.55, we can see that the large, classical field does not couple to the mechanical mode, as it does not create any phonon in the membrane. Its only role is to enhance the optomechanical interaction between the quantum fields $\delta\hat{a}^{(\dagger)}$ and $\hat{b}^{(\dagger)}$. This will allow us to externally modulate the coupling, to optimise the photon storage in the membrane.

In the interaction Hamiltonian eq.2.55, we can distinguish two characteristically different processes that can be brought into resonance by appropriately choosing the laser detuning Δ: parametric-down conversion and state-swap, (1) and (2) in eq.2.55, respectively. Both processes occur simultaneously, but for $\Omega_m\gg\kappa$ one of them dominates, with the other one being strongly suppressed [14].

Parametric-down conversion

We first look at to the left term (1) in the Hamiltonian eq.2.55, that becomes dominant by setting $\Delta=+\Omega_m$. The interaction Hamiltonian can be rewritten to be:

$$\hat{H}_{IM}\approx\hbar g\left[\delta\hat{a}^{\dagger}\hat{b}^{\dagger}+\delta\hat{a}\hat{b}\right] \tag{2.56}$$

This Hamiltonian describes a process where either a photon and a phonon are simultaneously created ($\hbar g\delta\hat{a}^\dagger\hat{b}^\dagger$), or annihilated ($\hbar g\delta\hat{a}^\dagger\hat{b}^\dagger$) with the help of the classical field.

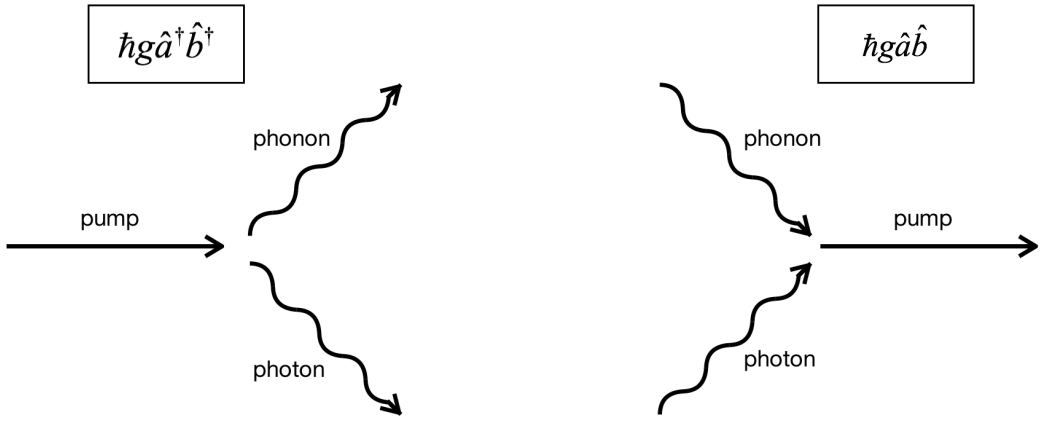

Figure 2.3: Parametric-down conversion process in an optomechanical cavity with an input consisting of strong field plus a quantum state.

This process is called *blue-sideband operation*, or *parametric-down conversion.*

State-swap

On the other hand, by setting $\Delta = -\Omega_m$ the second term (2) in eq.2.55 dominates, and the interaction Hamiltonian becomes:

$$\hat{H}_{IM} \approx \hbar g \left[\delta\hat{a}\hat{b}^\dagger + \delta\hat{a}^\dagger\hat{b}\right] \tag{2.57}$$

In this case, we no longer have a photon and a phonon created or annihilated at a time. On the contrary, in this regime we can either have a phonon created by annihilating a photon, or the opposite process.

This process is called *red-sideband operation*, or *state-swap.* The storage and retrieval of a photonic quantum state into a phononic state will be achieved through this process.

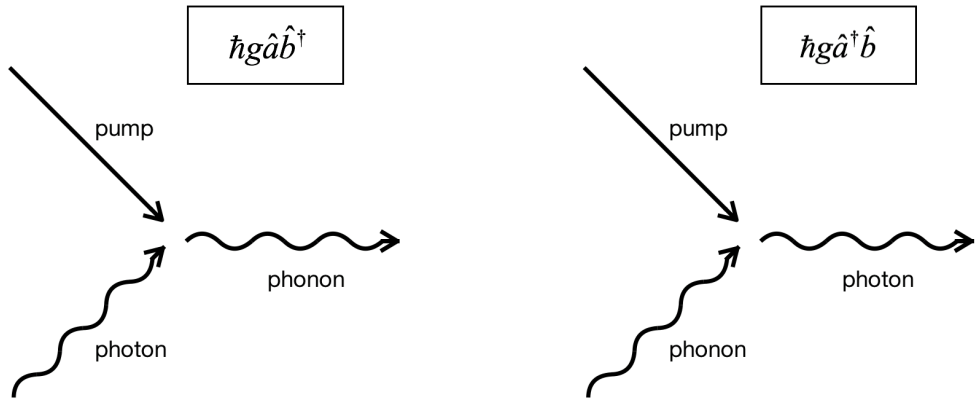

Figure 2.4: State-swap process in an optomechanical cavity with an input consisting of strong field plus a quantum state.

Chapter 3

First approach: the dirty experiment

For studying optomechanical quantum memories, we first analyse how does a membrane inside a cavity behave. Our aim is to store a single photon in the membrane's oscillating movementby sending towards the cavity the single photon plus a strong, classical field. This classical field effectively enhances the optomechanical coupling between the single photon quantum field and the mechanical modes in the membrane, and thus it gives us a way to tune the storage.

In this thesis, we stick to single photons, pumping classical fields and optomechanical cavities. In this chapter, however, we restrict ourselves to the study of the membrane's momentum, without taking into account the quantum dynamics of the phononic excitation. We consider some approximations, stated, justified and clarified in the following. In this order, we will:

1. Linearise the light fields.
2. Adiabatically eliminate the field inside the cavity.
3. Assume the incoming field to be a short pulse, to stress the adiabatic condition.

Finally, we find the time evolution of the momentum of the membrane, to have a first idea of what is happening in the mechanical part of our cavity, that constitutes the storage unit of our quantum memory.

3.1 Derivation of the expression for the membrane's momentum

Consider the general description of an optomechanical cavity with a moving mirror or membrane. Such a system is described by the Langevin equations of motion

$$\frac{d\hat{a}\left(t\right)}{dt} = -\left(\frac{\kappa}{2} + i\Delta\right)\hat{a}\left(t\right) + \sqrt{\kappa}\hat{a}_{in}\left(t\right) - G\hat{a}\left(t\right)\hat{x}\left(t\right), \tag{3.1}$$

$$\frac{d\hat{p}\left(t\right)}{dt} = -m\Omega_m^2\hat{x}\left(t\right) - \gamma\hat{p}\left(t\right) + \frac{m\Omega_m}{2}G\hat{a}^{\dagger}\left(t\right)\hat{a}\left(t\right) + \hat{F}_b\left(t\right), \tag{3.2}$$

$$\frac{d\hat{x}\left(t\right)}{dt} = \frac{1}{m}\hat{p}\left(t\right), \tag{3.3}$$

where the constants m and Ω_m are, respectively, the mass and the resonance frequency of the membrane, and κ and γ are the leak out and decay rates. Eq.3.1 describes the creation of photons inside the cavity, while eq.3.2 and eq.3.3 describe the momentum and position of the membrane. The operator $\hat{a}_{in}\left(t\right)$ is the input field sent in the cavity, and $\hat{F}_b\left(t\right)$ is the Langevin noise force.

3.1.1 Linearisation of the light fields

As stated earlier, we are interested in the case where we send a single photon (whose information we want to be stored) plus a strong, coherent field (which we want to use as control of the storage process in our memory). With this in mind, we linearise the equations of motion presented above, eq.3.1-3.3. The field operators $\hat{a}\left(t\right)$ and $\hat{a}_{in}\left(t\right)$ are thus rewritten:

$$\hat{a}\left(t\right) = \langle\hat{a}\left(t\right)\rangle + \delta\hat{a}\left(t\right) \tag{3.4}$$

$$\hat{a}_{in}\left(t\right) = \langle\hat{a}_{in}\left(t\right)\rangle + \delta\hat{a}_{in}\left(t\right) \tag{3.5}$$

where $\| \langle\hat{a}\left(t\right)\rangle \| \gg \|\delta\hat{a}\left(t\right)\|$ and $\| \langle\hat{a}_{in}\left(t\right)\rangle \| \gg \|\delta\hat{a}_{in}\left(t\right)\|$, so that the fields are assumed to be its mean plus a small perturbation.

If we now look at the input field after the linearisation is considered, eq.3.5, we can indeed see that this is a good description of the strong, classical field plus a single photon that we have discussed above. This linearisation is then, in the case we are interested in, the most convenient way to precisely describe our input field.

From now on, let us now change the notation used here to a more convenient one, by defining:

$$\alpha\left(t\right) \equiv \left\langle \hat{a}_{in}\left(t\right)\right\rangle \tag{3.6}$$

$$\hat{a}_{in}\left(t\right) \equiv \delta\hat{a}_{in}\left(t\right) \tag{3.7}$$

Regarding the field inside the cavity $\hat{a}\left(t\right)$, we can split its equation of motion, eq.3.1 in two contributions: the evolution of the mean field $\left\langle \hat{a}\right\rangle$ and the evolution of the small perturbation, $\delta\hat{a}$. According to this, and with the new notation stated above, the dynamics of the field inside the cavity can be expressed as:

$$\frac{d\left\langle \hat{a}\right\rangle}{dt} = -\left(\frac{\kappa}{2} + i\Delta\right)\left\langle \hat{a}\right\rangle + \sqrt{\kappa}\alpha\left(t\right) - G\hat{x}\left(t\right)\left\langle \hat{a}\right\rangle \tag{3.8}$$

$$\frac{d}{dt}\delta\hat{a}\left(t\right) = -\left(\frac{\kappa}{2} + i\Delta\right)\delta\hat{a}\left(t\right) + \sqrt{\kappa}\hat{a}_{in}\left(t\right) - G\hat{x}\left(t\right)\delta\hat{a}\left(t\right) \tag{3.9}$$

3.1.2 Adiabaticity condition and solutions

Above we derived the equations of motion for the field inside the cavity, eq.3.8 and eq.3.9. The momentum and position of the membrane are described in eq.3.2 and eq.3.3, respectively. Since these equations are coupled, we first solve for the field inside the cavity, eq.3.8 and eq.3.9, and later consider the mechanics.

Being this chapter a first attempt for studying the system, we restrict ourselves to the adiabatic regime only. The light field inside the cavity is assumed to change slowly with respect to the characteristic time κ of the cavity. In other words, the decoherence and leaking times need to be large enough to neglect the derivatives on the left hand side of eq.3.8 and eq.3.9. This adiabaticty condition, then, reads:

$$T_{\psi}^{-1} \ll \kappa, \tag{3.10}$$

where T_{ψ} is the characteristic time of the experiment. In this regime, the solutions to the field inside the cavity are:

$$\left\langle \hat{a}\left(t\right)\right\rangle = \sqrt{\kappa}\alpha\left(t\right)\left(\frac{\kappa}{2} + i\Delta + G\hat{x}\left(t\right)\right)^{-1}, \tag{3.11}$$

$$\delta\hat{a}\left(t\right) = \sqrt{\kappa}\hat{a}_{in}\left(t\right)\left(\frac{\kappa}{2} + i\Delta + G\hat{x}\left(t\right)\right)^{-1}. \tag{3.12}$$

3.1.3 Short pulse condition for the incoming field

When the incoming field enters the cavity, the membrane is kicked and its momentum and position change according to eq.3.2 and eq.3.3.

If this process is smooth and slow, one would need to solve both these equations in order to exactly know the time evolution of the membrane's quadratures. On the other hand, if one assumes that the light gives a fast kick to the membrane, this process is fast enough to let us ignore the change in position of the membrane.

Relating the physical parameters of the light fields and the cavity, this translates into the condition:

$$T_\psi \ll \Omega_m^{-1}, \gamma^{-1}, \tag{3.13}$$

where Ω_m is the characteristic frequency of the membrane and T_ψ is the pulse duration.

In the regime identified by the condition eq.3.13, we can neglect the movement of the membrane within the optical pulse and consider the mechanical system to be steady. To derive easy expressions, we also ignore the decay and noise terms, γ and $\hat{F}_b$ respectively. Thus, we rewrite the equations of motion for the mechanical part of the system within an optical pulse of duration T_ψ as:

$$\frac{d\hat{p}}{dt} = \frac{m\Omega_m}{2} G \left(\| \langle \hat{a} \rangle \|^2 + \langle \hat{a} \rangle \, \delta\hat{a}^\dagger + \langle \hat{a} \rangle^* \, \delta\hat{a} \right) \tag{3.14}$$

for the membrane's momentum, and

$$\frac{d\hat{x}}{dt} = 0 \tag{3.15}$$

for its position. It is important to emphasize that eq.3.15 is only valid within the pulse duration.

Since eq.3.15 for the mechanical position is trivial, from now on we do not consider the operator $\hat{x}(t)$, but a classical variable $x(t)$ instead. The position $x(t)$, as we have already justified, is considered to be steady in the timescales of our experiment. Without any interaction from the mechanical reservoir, we can assume that the oscillator has a sinusoidal dynamics, so that at the initial time t_0 the position of the membrane is $x(t_0) = A cos(\Omega_m t_0)$.

From eq.3.14 we can see that the momentum dynamics is completely determined by the light field inside the cavity. By plugging the solutions for the fields in the adiabatic regime eq.3.11 and eq.3.12 into the equation of motion of the operator $\hat{p}(t)$, eq.3.14, we find that

the membrane's momentum evolves according to:

$$\frac{d\hat{p}\left(t\right)}{dt}=\frac{m\Omega_m}{2}\frac{G\kappa}{\left(\frac{\kappa}{2}+gx\left(t_0\right)\right)^2+\Delta^2}\left[\left\|\alpha\left(t\right)\right\|^2+\alpha\left(t\right)\left(\hat{a}_{in}\left(t\right)+\hat{a}_{in}^{\dagger}\left(t\right)\right)\right]. \tag{3.16}$$

We thus have an expression describing the momentum of the membrane as a function of the incoming field (recall that $\alpha\left(t\right)$ is the large, classical, coherent field, and $\hat{a}_{in}\left(t\right)$ the single photon).

Let us now assume that the membrane is in its equilibrium position at $t=t_0$, so that the term $x\left(t_0\right)$ vanishes in the expression above, eq.3.16. Moreover, for sake of simplicity we introduce the constant:

$$P=\frac{m\Omega_m}{2}\frac{G\kappa}{\frac{\kappa^2}{4}+\Delta^2}. \tag{3.17}$$

By solving the equation of motion eq.3.16, we finally get:

$$\hat{p}\left(t_0+\Delta t\right)=P\int_{t_0}^{t_0+\Delta t}dt\left[\left\|\alpha\left(t\right)\right\|^2+\alpha\left(t\right)\left(\hat{a}_{in}\left(t\right)+\hat{a}_{in}^{\dagger}\left(t\right)\right)\right], \tag{3.18}$$

with which we find the change of momentum of the membrane, given an input field. One should be careful here and recall that, to reach this solution, we took some assumptions. For this solution to be valid, Δt has to fulfill the conditions of adiabaticity, eq.3.10, and short pulse, eq.3.13. Namely, this last expression will only describe our system correctly for times that can be comparable to the incoming pulse timescale:

$$\Delta t\sim T_\psi \tag{3.19}$$

Eq.3.18 can be used to determine the momentum change at any instant during the pulse, $\Delta t<T_\psi$. With that, it is possible to find the new oscillatory motion of the membrane, at least until the mechanical reservoir perturbs the dynamics (this is, for a timescale t such that $t\ll\gamma^{-1}$).

3.2 Computation of $\langle\hat{p}^2\rangle$

When studying mechanical systems, one of the most important and interesting properties is the momentum, with which we can compute the kinetic energy. In quantum mechanics, however, since the square of the expected value of an observable is not equal to the expected value of its square, we have to directly compute $\langle\hat{p}^2\rangle$. In this section, we will make use of the equation for the momentum of the membrane derived above, eq.3.18, and study how it changes when we send different pulses.

In particular, we are interested in the net effect of the single photon on the membrane's momentum, computed as the difference in momentum that it experiences when we consider two consecutive pulses. We first send the classical field plus the single photon. Later on, after half a mechanical period, and always in a timescale fulfilling the conditions stated earlier in order to the derived equation to be valid, we send a second, equally shaped classical pulse, without the single photon.

3.2.1 First pulse: classical field plus a single photon

As we have discussed above, we send towards the cavity a classical pulse plus a single photon. Let us define more carefully how this fields look like. First, the classical field carries a certain number of photons, distributed with a certain shape in time:

$$\alpha(t) = \sqrt{N} f(t). \tag{3.20}$$

Here N is the number of photons in the field, and $f(t)$ is a normalisation function, such that:

$$\int_{-\infty}^{+\infty} dt \|\alpha(t)\|^2 = N. \tag{3.21}$$

On the other hand, the single photon will be described by a density matrix of the form:

$$\hat{\rho}_1 = (1-q)|0\rangle\langle 0| + q\hat{a}_\psi^\dagger |0\rangle\langle 0|\hat{a}_\psi \tag{3.22}$$

where a single photon is created with a probability q and a certain wave function, this is:

$$\hat{a}_\psi = \int_{-\infty}^{+\infty} dt \psi(t)\hat{a}. \tag{3.23}$$

The wave function $\psi(t)$ is also normalised, as it describes an input pulse with a single photon.

Since $\alpha(t)$ describes a classical field, it enters directly in the equation for the time evolution of $\hat{p}(t)$, eq.3.18, and our computation finally resumes to:

$$Tr\{\hat{\rho}_1\hat{p}^2\} = (1-q)\langle 0|\hat{p}^2|0\rangle + q\langle 0|\hat{a}_\psi\hat{p}^2\hat{a}_\psi^\dagger|0\rangle \tag{3.24}$$

Let us compute the outcome of eq.3.24 by parts. For the first average, $\langle 0|\hat{p}^2|0\rangle$, we find:

$$\langle 0|\hat{p}^2|0\rangle =$$

$$= P^2 \int_{t_0}^{t_0+\Delta t} dt' \int_{t_0}^{t_0+\Delta t} dt'' \langle 0|\left[\|\alpha(t')\|^2 + \alpha(t')\left(\hat{a}_{in}(t') + \hat{a}_{in}^\dagger(t')\right)\right]$$

$$\left[\|\alpha\left(t''\right)\|^2+\alpha\left(t''\right)\left(\hat{a}_{in}\left(t''\right)+\hat{a}_{in}^{\dagger}\left(t''\right)\right)\right]|0\rangle=$$

$$=P^2\int_{t_0}^{t_0+\Delta t}dt'\int_{t_0}^{t_0+\Delta t}dt''\left[N^2\|f\left(t'\right)\|^2\|f\left(t''\right)\|^2+Nf\left(t'\right)f^*\left(t''\right)\underbrace{\langle 0|\,\hat{a}\left(t'\right)\hat{a}^{\dagger}\left(t''\right)|0\rangle}_{\delta(t'-t'')}\right]=$$

$$=P^2\left[N^2+N\right] \tag{3.25}$$

Recall that, according to the condition stated earlier in eq.3.19, we assumed that the timescale of this process was comparable to the timescale of the incoming pulse. In this last result, eq.3.25, we made this condition a bit more strict: we assume that, during Δt, the whole pulse enters the cavity and interacts with the membrane, this is, $\Delta t \geq T_{\psi}$, so that we make sure that all its energy is transferred to the mechanical system. Thus, the coherent pulse's time distribution function, $f\left(t\right)$, is normalised in the timespan $[t_0, t_0+\Delta t]$.

Finally, for the second braket in eq.3.24, $\langle 0|\,\hat{a}_{\psi}\hat{p}^2\hat{a}_{\psi}^{\dagger}\,|0\rangle$, we find:

$$\langle 0|\,\hat{a}_{\psi}\hat{p}^2\hat{a}_{\psi}^{\dagger}\,|0\rangle=$$

$$=P^2\int_{t}^{t+\Delta t}dt'\int_{t}^{t+\Delta t}dt''\int_{-\infty}^{+\infty}d\tau_1\int_{-\infty}^{+\infty}d\tau_2\psi^*\left(\tau_1\right)\psi\left(\tau_2\right)$$

$$\langle 0|\,\hat{a}\left(\tau_1\right)\Big\{N^2f\left(t'\right)^2f\left(t''\right)^2+Nf\left(t'\right)f\left(t''\right)\hat{a}^{\dagger}\left(t'\right)\hat{a}\left(t''\right)+Nf\left(t'\right)f\left(t''\right)\hat{a}\left(t'\right)\hat{a}^{\dagger}\left(t''\right)\Big\}\hat{a}^{\dagger}\left(\tau_2\right)|0\rangle=$$

$$=P^2\int_{t}^{t+\Delta t}dt'\int_{t}^{t+\Delta t}dt''\int_{-\infty}^{+\infty}d\tau_1\int_{-\infty}^{+\infty}d\tau_2\psi^*\left(\tau_1\right)\psi\left(\tau_2\right)\Big\{N^2f\left(t'\right)^2f\left(t''\right)^2\delta\left(\tau_1-\tau_2\right)+$$

$$+Nf\left(t'\right)f\left(t''\right)\delta\left(t'-\tau_1\right)\delta\left(t''-\tau_2\right)+Nf\left(t'\right)f\left(t''\right)\Big[\delta\left(t'-t''\right)\delta\left(\tau_1-\tau_2\right)+\delta\left(t''-\tau_1\right)\delta\left(t'-\tau_2\right)\Big]\Big\}=$$

$$=P^2\Big\{N^2+N\left(1+2\Lambda\right)\Big\} \tag{3.26}$$

where we defined Λ as the scalar product between the distribution function of the coherent pulse, and the single photon's wave function:

$$\Lambda = \left\| \int_{-\infty}^{+\infty} dt f^{*}(t)\, \psi(t) \right\|^{2} \tag{3.27}$$

In chapter 4, we consider the fully quantum description of our system, and we will find out that this overlap between the time distributions of the single photon and the coherent pulse is crucial for the storage and retrieval optimisation of the information in our memory.

Gathering both results eq.3.25 and eq.3.26 together, we conclude that the expected value of the squared momentum operator in the cavity's membrane, at a time $t = t_0 + \Delta t$, with $\Delta t \gtrsim T_\psi$, is:

$$\langle \hat{p}^2 \rangle = \left(\frac{m\Omega_m}{2} \right)^2 \frac{G^2\kappa^2}{\frac{\kappa^2}{4} + \Delta^2} \left[N^2 + N(1 + 2q\Lambda) \right]. \tag{3.28}$$

3.2.2 Second pulse: classical field alone and variations in $\langle \hat{p}^2 \rangle$

Above we computed the membrane's squared momentum due to the first pulse. After half a mechanical period we send in the cavity a second pulse, consisting only in the classical field, with the same time distribution $f(t)$ used before. We are interested in the total variation in $\langle \hat{p}^2 \rangle$ after these two consecutive pulses. So, in the same way done above, we now consider an incoming quantum field described by a vacuum density matrix:

$$\hat{\rho}_2 = |0\rangle \langle 0|. \tag{3.29}$$

We use the same technique for determining the change of amplitude due to the second, classical pulse. Then, by summing these contributions together, we find the net effect of the single photon to be:

$$\Delta \langle \hat{p}^2 \rangle = \left(\frac{m\Omega_m}{2} \right)^2 \frac{G^2\kappa^2}{\left(\frac{\kappa^2}{4} + \Delta^2 \right)^2} N 2q\Lambda. \tag{3.30}$$

For experimental purposes, we are interested to express eq.3.30 with the physical parameters of the system. In particular, in experimental physics the losses in the cavity are related to the finesse $\mathcal{F}$. This is defined as the cavity's free spectral range divided by the (full width at half maximum) bandwith of its resonances. In general, if we define r as the fraction of power left inside the cavity after one round trip (so that $1 - r$ is the fraction lost) the finesse of a cavity is given by [6]:

$$\mathcal{F} = \frac{\pi}{2 \arcsin\left(\frac{1-\sqrt{r}}{2\sqrt[4]{r}} \right)} \approx 2\frac{\pi}{1-r}. \tag{3.31}$$

Importantly, the finesse is fully characterised by the cavity's losses, and completely independent of its length. Additionally, we can relate the constants κ and G appearing in eq.3.30 as [14]:

$$\kappa = \frac{c}{2L}(1-r), \tag{3.32}$$

$$G = \frac{\pi c}{L^2} x_{ZPM}^2, \tag{3.33}$$

where c is the speed of light in vacuum. Recall that we considered a system with only one moving mirror, and with only one mechanical degree of freedom. Other geometries can, in general, present different linear optomechanical coupling rates, but we will restrict ourselves to the study of systems fulfilling this description.

Finally, we put everything together and, for sake of simplicity, assume the system to be in a near resonance regime, so that $\Delta \ll \kappa$. Moreover, we consider an ideal single photon source, such that $q = 1$. Then, the variation in the expected squared momentum of the membrane due to the single photon is:

$$\Delta \langle \hat{p}^2 \rangle = 8 \left(\frac{m\Omega_m x_{ZPM}^2}{L} \right)^2 \mathcal{F}^2 N \Lambda \tag{3.34}$$

With this last expression, we understand how the strong classical field enhances the momentum transfer between the single photon and the cavity's membrane. We summarise the results of this chapter:

- From the definition of Λ in eq.3.27, and eq.3.34 we find that the transfer of momentum is proportional to the scalar product between the two fields $f(t)$ and $\psi(t)$. This transfer is thus maximised when their distributions match. For a certain number of photons, the more similar the distributions are to each other, the better will be the momentum transfer.

- If we want to increase the resolution of our experiment, we only need to use a larger number of photons N in our classical field.

- To a higher finesse is associated a higher momentum transfer

Chapter 4

An optomechanical quantum memory

In chapter 3 we introduced the problem of an optomechanical quantum memory in which we want to store a single photon with the help of a classical coherent field, by studying the dynamics of the membrane from a classical point of view. In the following, we consider the quantisation of both the electromagnetic field and the vibrational modes of the cavity. Thus, we deal with the fully quantised hamiltonian, with the creation and anihilation operators for phonons, $\hat{b}^\dagger$ and $\hat{b}$. We assume the system to be red-detuned from the cavity resonance frequency, so that the Hamiltonian, after linearising the optical field inside the cavity, is:

$$\hat{H} = \hbar\Delta\hat{a}^\dagger\hat{a} + \Omega_m\hat{b}^\dagger\hat{b} + \hbar g\left(\hat{a}^\dagger\hat{b}\alpha^* + \hat{a}\hat{b}^\dagger\alpha\right). \tag{4.1}$$

Here $\hat{a}$ describes the small perturbation in the light field inside the cavity, while α is the large, classical field inside the cavity. From this Hamiltonian, we derive the equations of motion for $\hat{a}$ and $\hat{b}$:

$$\dot{\hat{b}} = -ig\alpha\hat{a}, \tag{4.2}$$

$$\dot{\hat{a}} = -\left(\frac{\kappa}{2} + i\Delta\right)\hat{a} - ig\alpha^*\hat{b} + \sqrt{\kappa}\hat{a}_{in}, \tag{4.3}$$

where we switched to a rotating frame where Δ is the detuning from the characteristic frequency $\omega_L - \Omega_m$ of the red sideband. It is important to state that in this work we restrict ourselves to systems without decoherence in the mechanical modes. With this we mean that the timescale of the dynamics we are interested in, is much shorter than the characteristic mechanical lifetime. This fact allows us to exclude extra terms in the equation of motion for the operator $\hat{b}(t)$. We take it as a postulate, without any demonstrations. Further work and discussions towards this direction might be interesting to explore.

Using the same notation introduced in previous chapters, $\hat{a}_{in}$ describes the incoming single photon.

In order to completely describe the dynamics of the system, in addition to equations 4.2 and 4.3, we need the input-output relation for the optical field

$$\hat{a}_{out} = -\sqrt{\kappa}\hat{a} + \hat{a}_{in}. \tag{4.4}$$

In this chapter, we make use of the Hamiltonian of eq.4.1 to study the storage of the single photon in the mechanical mode. Our goal is to find the maximum achievable efficiency. In order to do so, we first solve the system numerically, to gain an insight of *what* is happening. We compare our results with the ones obtained in [7]. Later on, in order to understand *why* this is happening, we develop an analytical theory that pushes the adiabatic elimination to higher orders. We compare our results with the numerics to make a validity check. In the analytical study, we first consider the adiabatic regime, for which the adiabatic approximation is valid. We optimise the shape of the large pulse to achieve the maximum efficiency in the photon storage in this regime. Then, we study the non-adiabatic regime starting with the same optimal pulse shape, and use our theory to determine corrections to the efficiency.

4.1 Numerical approach

In this section we numerically investigate the exact solutions to the output field and the phonon dynamics in the membrane, eq.4.4 and 4.2, respectively. This way, we determine the excitations created in the membrane, which correspond to the number of photons stored in our memory. Later on, we compute the storage efficiency by comparing this number with the number of photons sent towards it (in our case, this last number will be always one, but this numerics can be used for higher number of photons). In the following, we describe the numerical method we use. All the numerical plots presented in this thesis are derived with the method presented in this section.

To begin with, we write down the most general solutions for the operators describing the phonon dynamics and the output field. Since both operators are described by linear equations of motion, eq.4.4 and 4.2, we know that the form of the solutions for $\hat{b}(t)$ and $\hat{a}_{out}(t)$ can be expressed as:

$$\hat{b}(t) = c(t)\,\hat{b}(0) + \int_0^t dt' f\left(t'\right)\hat{a}_{in}\left(t'\right), \tag{4.5}$$

$$\hat{a}_{out}(t) = h(t)\,\hat{b}(0) + \int_0^t dt' g\left(t,t'\right)\hat{a}_{in}\left(t'\right), \tag{4.6}$$

where $c(t)$, $f(t)$, $h(t)$, $g(t,t')$ are functions to be found numerically. Since it is hard to work with operators, we assume the system to be in coherent states. The response of the system for single photon inputs is thus recovered by recalling the linearity property of quantum mechanics, and the completeness of the set of coherent states. Equations 4.5 and 4.6 can thus be written as

$$b(t) = c(t)\, b(0) + \int_0^t dt' f\left(t'\right) \psi\left(t'\right), \tag{4.7}$$

$$a_{out}(t) = h(t)\, b(0) + \int_0^t dt' g\left(t,t'\right) \psi\left(t'\right), \tag{4.8}$$

where $\psi(t)$ has to be intended as the wave function of the single photon. We can now plug eq.4.7 and eq.4.8 in the equations of motion derived earlier, eqs.4.2-4.4 to have a system of differential equations suitable for a numerical analysis. What we want to do is, essentially, to express our equations of motion in terms of the functions $c(t)$, $f(t)$, $h(t)$, $g(t,t')$ only.

By plugging the general solution for the operator $b(t)$, eq.4.7, into the equation of motion describing the phonon dynamics, eq.4.2, we find a differential equation in terms of the new functions $c(t)$ and $f(t)$:

$$\dot{c}(t)\, b(0) + f(t)\, \psi(t) = -ig\alpha(t)\, a(t). \tag{4.9}$$

Since we do not have a solution for the light field $a(t)$ in terms of the functions we want to solve numerically for, we use the input-output relation introduced earlier to find:

$$a(t) = \frac{\psi(t)}{\sqrt{\kappa}} - \frac{h(t)\, b(0)}{\sqrt{\kappa}} - \int_0^t dt' \frac{g(t,t')\, \psi(t')}{\sqrt{\kappa}}. \tag{4.10}$$

Plugging this last result, eq.4.10, in the equation of motion for the coefficients, eq.4.9, we derive an equation that only depends on the functions $c(t)$, $f(t)$, $h(t)$, $g(t,t')$:

$$\dot{c}(t)\, b(0) + f(t)\, \psi(t) = ig\frac{\alpha(t)}{\sqrt{\kappa}} \int_0^t dt' g\left(t,t'\right) \psi\left(t'\right) + ig\frac{\alpha(t)}{\sqrt{\kappa}} h(t)\, b(0) - ig\frac{\alpha(t)}{\sqrt{\kappa}} \psi(t). \tag{4.11}$$

Focusing our attention to this last result, eq.4.11, we distinguish two different contributions. First, we recognise the terms related to the mechanics: those having some relation with the operator $b(0)$. Second, the terms taking into account the single photon input field, $\psi(t)$. One can claim that the evolution of these different contributions needs to be independent from each other. In other words, we can decouple eq.4.11 into a mechanical contribution, and a single photon contribution $\psi(t)$, to find:

$$\dot{c}(t) = ig\frac{\alpha(t)}{\sqrt{\kappa}} h(t), \tag{4.12}$$

$$f(t) = ig\frac{\alpha(t)}{\sqrt{\kappa}}\frac{G(t)}{\psi(t)}. \tag{4.13}$$

Here, we defined the function

$$G(t) = \int_0^t dt' g\left(t,t'\right)\psi\left(t'\right) - \psi(t). \tag{4.14}$$

From the equation of motion of the operator $\hat{b}(t)$, eq.4.2, we found two equations relating the four functions we want to solve numerically for. If we apply the same procedure again for the equation of motion of the field inside the cavity, eq. 4.3, we can use similar arguments to find the other two equations:

$$\dot{h}(t) = -\left(i\Delta + \frac{\kappa}{2}\right)h(t) + ig\sqrt{\kappa}\alpha^*(t)\,c(t), \tag{4.15}$$

$$\dot{G}(t) = -\left(i\Delta + \frac{\kappa}{2}\right)G(t) - g^2\alpha^*(t)\int_0^t dt' G\left(t'\right)\alpha\left(t'\right) - \kappa\psi(t). \tag{4.16}$$

For practical purposes, we rewrite this last equation by making the substitution $I(t) = \int_0^t dt' G(t')\,\alpha(t')$ in eq.4.16:

$$\dot{G}(t) = -\left(i\Delta + \frac{\kappa}{2}\right)G(t) - g^2\alpha^*(t)\,I(t) - \kappa\psi(t). \tag{4.17}$$

The function $I(t)$ thus satisfies

$$\dot{I}(t) = G(t)\,\alpha(t). \tag{4.18}$$

In order to write the system in a more compact way, we collect the four ordinary differential equations in matrix notation:

$$\begin{bmatrix} \dot{c}(t) \\ \dot{G}(t) \\ \dot{h}(t) \\ \dot{I}(t) \end{bmatrix} = \begin{bmatrix} 0 & 0 & ig\frac{\alpha(t)}{\sqrt{\kappa}} & 0 \\ 0 & -\left(\frac{\kappa}{2}+i\Delta\right) & 0 & -g^2\alpha^*(t) \\ ig\sqrt{\kappa}\alpha^*(t) & 0 & -\left(\frac{\kappa}{2}+i\Delta\right) & 0 \\ 0 & \alpha(t) & 0 & 0 \end{bmatrix} \begin{bmatrix} c(t) \\ G(t) \\ h(t) \\ I(t) \end{bmatrix} + \begin{bmatrix} 0 \\ -\kappa\psi(t) \\ 0 \\ 0 \end{bmatrix} \tag{4.19}$$

From the definitions of the coefficients $c(t)$, $G(t)$, $h(t)$, $I(t)$, it is possible to determine their initial values:

$$\begin{bmatrix} c(0) \\ G(0) \\ h(0) \\ I(0) \end{bmatrix} = \begin{bmatrix} 1 \\ -\psi(0) \\ 0 \\ 0 \end{bmatrix}. \tag{4.20}$$

We solve the system in eq.4.19 with the initial conditions in eq.4.20 with the non stiff, versatile ode solver `ode45` [8] available in MATLAB®'s library, which is based on an explicit Runge-Kutta (4,5) formula, the Dormand-Prince pair [9][10]. With this, and adding the relation with the last function, $f(t)$, eq.4.13 we find a solution and can check the theoretical results derived in the following.

4.2 Analytic solution and optimisation in the adiabatic regime

We now study our system analytically, comparing our results with the ones obtained with the numerical method derived in the previous section. Here, we derive the optimal shape of the strong pulse for the photon storage in the adiabatic limit. This guarantees that, at least in the adiabatic regime, the storage efficiency of our memory is maximised.

As we justified in the previous chapter, we can adiabatically eliminate the field inside the cavity if the leaking out time described by the constant κ is large enough compared to the time evolution of the light fields. The condition to be fulfilled is :

$$\kappa\sigma \gg 1, \tag{4.21}$$

where σ is the timescale characterising the single photon, and is required to be shorter than the pulse duration T_ψ. For instance, σ could be the width of a Gaussian pulse. This condition is the same as the one given in the previous chapter, but written in a more convenient way. As we shall see later on, eq.4.21 is indeed fully characterising the adiabaticity of the system.

4.2.1 Storage and retrieval of information in the membrane

Assuming the condition eq.4.21 to be fulfilled, we can find the adiabatic solution to the field inside the cavity to be:

$$\hat{a}\left(t\right) = \frac{-ig\alpha^{*}\left(t\right)\hat{b}\left(t\right) + \sqrt{\kappa}\hat{a}_{in}\left(t\right)}{\frac{\kappa}{2} + i\Delta} \tag{4.22}$$

Using the equation of motion for the operator $\hat{b}\left(t\right)$, eq.4.2, and the adiabatic solution to the field inside the cavity, eq.4.22, the phonon dynamics can be derived from the differential equation:

$$\dot{\hat{b}}\left(t\right) = -\hat{b}\left(t\right)\frac{g^{2}\|\alpha\left(t\right)\|^{2}}{\frac{\kappa}{2} + i\Delta} - ig\frac{\sqrt{\kappa}}{\frac{\kappa}{2} + i\Delta}\alpha\left(t\right)\hat{a}_{in}\left(t\right) \tag{4.23}$$

This equation can be formally integrated to find the time evolution of the phonon creation operator, yielding:

$$\hat{b}\left(t\right) = \hat{b}\left(0\right)e^{-\gamma(t)} - ig\frac{\sqrt{\kappa}}{\frac{\kappa}{2} + i\Delta}\int_{0}^{t} dt'\alpha\left(t'\right)\hat{a}_{in}\left(t'\right)e^{\gamma(t')-\gamma(t)}, \tag{4.24}$$

where we defined:

$$\gamma\left(t\right) = \frac{g^{2}}{\frac{\kappa}{2} + i\Delta}\int_{0}^{t} dt'\|\alpha\left(t'\right)\|^{2}. \tag{4.25}$$

The mechanical creation and annihilation operators $\hat{b}^{(\dagger)}(t)$ given in eq.4.24 do satisfy the commutation relation:

$$\left[\hat{b}(t), \hat{b}^{\dagger}\left(t'\right)\right] = \delta\left(t - t'\right) \tag{4.26}$$

does hold for the derived expression for $\hat{b}(t)$ eq.4.24.

Let us take a closer look at eq.4.24 and the definition eq.4.25. Since $\gamma(t)$ is a positive, strictly increasing function, and $\alpha(t)$ is normalised to a certain number of photons N, at timescales large compared to the width σ of the coherent pulse $\alpha(t)$, the exponential term behaves like a Heaviside step function. For $t \gg \sigma$, then, the first term in eq.4.24 disappears, allowing us to explore not only the storage of photons in the mechanical modes, but also their retrieval (recall that we assumed an infinite decoherence time for the membrane's modes). This way, we see now the importance of the classical pulse's shape $\alpha(t)$.

Basically, if we want a fast and complete retrieval of the information stored, we have to send a classical pulse $\alpha(t)$ with a large number of photons within a short time (this is exactly the scenario explored in chapter 2, where we investigated the change in momentum due to a fast kick in the membrane). If these two parameters, namely the number of photons and the pulse duration are, respectively, large and short enough, the shape of the pulse will not matter and we can increase the efficiency and the speed of the retrieval process as much as desired.

If, on the other hand, we are interested in the storage of a new single photon, the shape of the strong, classical field does play a role. Therefore, we have to find the optimal pulse shape that maximises the efficiency of the storage process. We investigate this in the following section.

4.2.2 Optimisation of the pulse shape for storage purposes

Above we found the relation, in the adiabatic limit, between the creation of phonons in the membrane and the field inside the cavity. In this section, we optimise the shape of $\alpha(t)$ for storage purposes. In order to simplify our computations, we assume that our memory is in its ground state at the time we start our experiment (or, in other words, that no photon has been stored previously, so that we do not have to take into account the retrieval process before the storage of the new incoming field): $\hat{b}(0) = 0$.

As said above, we send a single photon and a classical field, and we want to store the first one. The total time of the experiment T_e is required to be longer than the single

photon pulse duration, T_ψ, so that we make sure that we send the whole pulse and all of its energy is transferred to the membrane's mechanical modes.

To quantify the storage efficiency, we compute the mean number of phonons in the membrane after we sent the pulse, and divide it by the number of photons we are interested in storing. In the following, we consider a single photon (such that only a single phonon can be created in the membrane), and thus the efficiency coincides with the mean number of phonons: $\eta = \langle \hat{n}_b \rangle = \langle \hat{b}^\dagger (T_e)\, \hat{b}\, (T_e) \rangle$.

Defining the incoming pulse as we did in previous chapters

$$\hat{a}_{in} = \int_{-\infty}^{+\infty} dt \psi\, (t)\, \hat{a}\, (t)\,, \tag{4.27}$$

we finally find, using eq.4.24, the mean number of phonons:

$$\langle \hat{n}_b \rangle = \|Z\|^2 e^{-\gamma^*(T_e)-\gamma(T_e)} \int_0^{T_e} dt' \int_0^{T_e} dt'' \int_{-\infty}^{+\infty} d\tau_1 \int_{-\infty}^{+\infty} d\tau_2$$

$$\psi\, (\tau_1)\, \psi^*\, (\tau_2)\, \alpha\, \left(t'\right) \alpha^*\, \left(t''\right) e^{\gamma^*(t')+\gamma(t'')} \underbrace{\langle 0|\, \hat{a}\, (\tau_1)\, \hat{a}^\dagger\, \left(t'\right) \hat{a}\, \left(t''\right) \hat{a}^\dagger\, (\tau_2)\, |0\rangle}_{\delta(\tau_1 - t')\delta(\tau_2 - t'')} =$$

$$= \left\| \int_0^{T_e} dt Z \alpha\, (t)\, \psi\, (t)\, e^{\gamma(t)-\gamma(T_e)} \right\|^2. \tag{4.28}$$

In this last expression, we introduced, for simplicity, the constant Z, which groups all the other ones in eq.4.24:

$$Z = -ig \frac{\sqrt{\kappa}}{\frac{\kappa}{2} + i\Delta} \tag{4.29}$$

If we want to maximise the photon storage, we can identify this last expression eq.4.28 as the scalar product between two appropriately defined functions. The first one, which we call the *control function* $\Upsilon\, (T_e, t)$, depends on the large field $\alpha\, (t)$ only (recall the definition of $\gamma\, (t)$, eq.4.25). Defined as

$$\Upsilon\, (T_e, t) = Z \alpha\, (t)\, e^{\gamma(t)} e^{-\gamma(T_e)}, \tag{4.30}$$

it describes how we can tune the efficiency of the process by changing the shape of $\alpha\, (t)$. The second function in the scalar product is the wave function $\psi\, (t)$ of the single photon, which we want to be stored in the phononic mode of the membrane.

Since the storage efficiency equals to the scalar product of two normalised functions (see

appendix A), we know, recalling the Cauchy-Bunyakovsky-Schwarz (CBS) theorem, that it will be upper limited by the product of its absolute values:

$$\left\| \int_0^{T_e} dt \Upsilon \left(T_e, t \right) \psi \left(t \right) \right\|^2 \leq 1. \tag{4.31}$$

Eq.4.31 is in agreement with the fact that the maximum expected number of phonons created in the membrane (and the maximum efficiency) equals one. The CBS theorem also states that the equality is reached if and only if

$$\Upsilon \left(T_e, t \right) = \psi^* \left(t \right). \tag{4.32}$$

Recalling the definitions of the control function $\Upsilon \left(T_e, t \right)$, eq.4.30, and $\gamma \left(t \right)$, eq.4.25, the optimal shape of the large field is found by solving the following integral equation:

$$\alpha \left(t \right) = \frac{\psi^* \left(t \right)}{Z} e^{\frac{g^2}{\frac{\kappa}{2} + i\Delta} \int_t^{T_e} dt' \| \alpha(t') \|^2}. \tag{4.33}$$

Tt is useful to take a look at the time variables involved in eq.4.33. T_e is a parameter that defines the experiment's final time, and t is the variable in which the experiment takes place, so that $0 < t < T_e$. With this in mind, let's find the solution to the integral equation, eq.4.33.

First, by taking the absolute values of both sides in eq.4.33 and rewriting the exponent, we get:

$$\| \alpha \left(t \right) \|^2 = \frac{\| \psi \left(t \right) \|^2}{\| Z \|^2} e^{\| Z \|^2 \int_t^{T_e} dt' \| \alpha(t) \|^2}. \tag{4.34}$$

Introducing the new variable $y \left(t, T_e \right)$, defined as:

$$y \left(t, T_e \right) = \int_t^{T_e} dt' \| \alpha \left(t' \right) \|^2, \tag{4.35}$$

$$\frac{\partial}{\partial t} y \left(t, T_e \right) = - \| \alpha \left(t \right) \|^2, \tag{4.36}$$

eq.4.34 can be rewritten as:

$$- \frac{\partial y \left(t, T_e \right)}{\partial t} = \frac{\| \psi \left(t \right) \|^2}{\| Z \|^2} e^{\| Z \|^2 y(t, T_e)}. \tag{4.37}$$

The boundary condition is $y \left(T_e, T_e \right) = 0$, as can be trivially found from the definition of $y \left(t, T_e \right)$. The solution is:

$$y \left(t, T_e \right) = - \frac{1}{\| Z \|^2} \log \left\{ 1 - \int_t^{T_e} \| \psi \left(t' \right) \|^2 dt' \right\}. \tag{4.38}$$

Substituting this solution into the first integral equation, eq.4.33, we find:

$$\alpha_0 \left(t \right) = \frac{\psi^* \left(t \right)}{Z} \left[1 - \int_t^{T_e} dt' \| \psi \left(t' \right) \|^2 \right]^{-\frac{1}{2} + i \frac{\Delta}{\kappa}}, \tag{4.39}$$

which is valid for any value of T_e. Importantly, as we discussed previously, the final experimental time T_e must be large enough to have the single photon pulse transferred into the membrane. Therefore, T_e must be (at least) large enough such that $\psi(t)$ is normalised over it:

$$\int_0^{T_e} dt \|\psi(t)\|^2 = 1. \tag{4.40}$$

By imposing this condition into eq.4.39, we finally find the shape that optimises the adiabatic storage of the single photon:

$$\alpha_0(t) = \frac{\psi^*(t)}{Z}\left[\int_0^t dt' \|\psi(t')\|^2\right]^{-\frac{1}{2}+i\frac{\Delta}{\kappa}}. \tag{4.41}$$

This result, for the case of zero detuning, $\Delta = 0$, is the same as the one found by *Gorshkov et al.* for the optimal adiabatic storage in a Λ-type optical dense atomic media [7].

4.2.3 Implications in the adiabatic limit

First by, if we want to perform the experiment described above, the physical parameter we would be interested in would be the light's intensity needed to maximise the storage of the single photon. This incoming intensity, $I(t)$, is proportional to the modulus squared of $\alpha(t)$ (which essentially tells us the instantaneous flux of photons within the classical pulse in the cavity).

$$I(t) = \|\alpha(t)\|^2. \tag{4.42}$$

The intensity needed to achieve a maximum storage efficiency is thus

$$I(t) = \frac{\frac{\kappa}{2}+\Delta^2}{g^2\kappa}\frac{\|\psi(t)\|^2}{\int_0^t \|\psi(t')\|^2}. \tag{4.43}$$

Importantly, the limits of $I(t)$ can be seen to be:

$$\lim_{t\to 0} I(t) = \infty, \tag{4.44}$$

$$\lim_{t\to T_e} I(t) = \frac{\frac{\kappa}{2}+\Delta^2}{g^2\kappa}\|\psi(T_e)\|^2. \tag{4.45}$$

It is interesting that, even if we assumed the mechanics to be initially in its ground state (or, equivalently, that no photon had been stored previously), we find that this incoming control pulse is not only optimal for the storage process, but also for the retrieval of any previously stored field. We can understand this fact more clearly if we plot the intensity $I(t)$, eq.4.43, and recalling the results of previous chapters: in chapter 2 we showed that, in order to achieve a maximum change in the membrane's momentum (without assuming any initial state for it), we need a large number of photons sent within the classical pulse.

In this case, and comparing the timescales of the intensity and the single photon pulse, we conclude that any information previously stored is retrieved before storing the new single photon. This fact can also be understood with a time reversal argument, as done in [7].

Fig.4.1 shows the intensity of the optimal pulse $\alpha_0(t)$ for a sinusoidal-shaped single photon, $\psi(t) = \left(\frac{2}{\pi}\right)^{\frac{1}{2}} sin(t)$, $0 \leq t \leq T_\psi$, with the pulse duration $T_\psi = \pi$ and the experimental time $T_e = 2T_\psi$. and the wave function of the single photon itself, so that the timescales of both functions can be compared. It is only used as qualitative proof of this behaviour, and thus the units of time and intensity are meaningless.

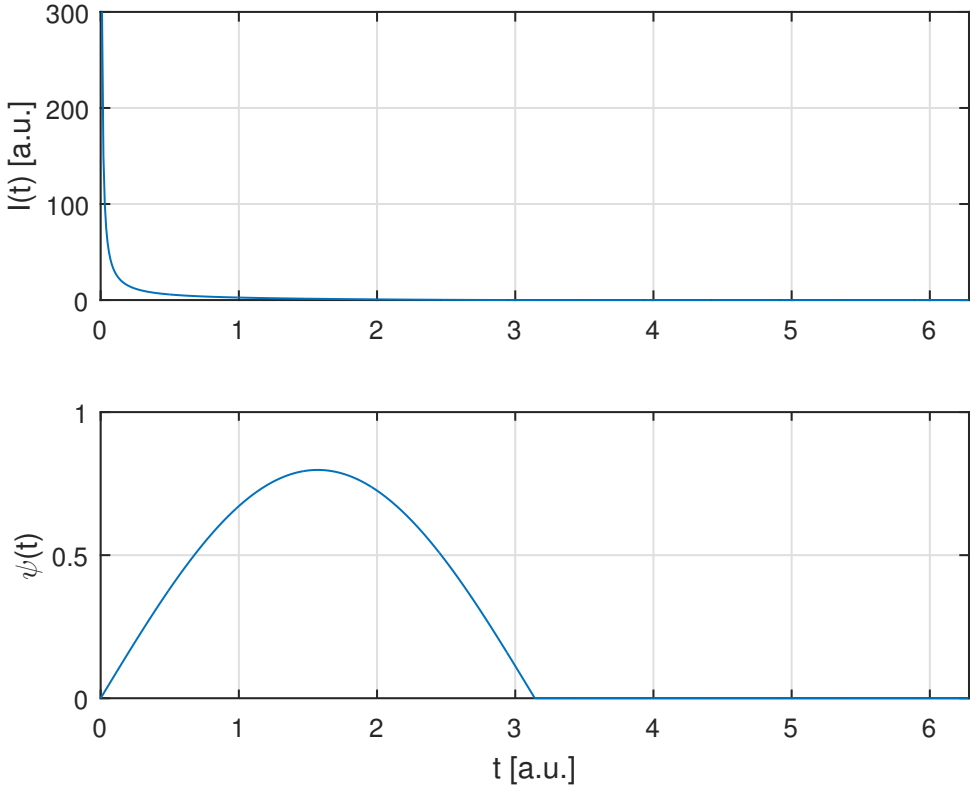

Figure 4.1: Intensity of the optimal control pulse $\alpha_0(t)$ (top plot) and single photon's shape $\psi(t)$ (bottom plot).

It is now a good exercise to make sure that the expression for $\alpha(t)$ derived above, eq.4.41, does maximise the stored number of photons in the membrane. In order to do so, let us compute the mean number of phonons in the membrane, eq.4.28, with the constraint

$\alpha(t) = \alpha_0(t)$.

$$\langle \hat{n}_b(T_e) \rangle = \left\| \int_0^{T_e} dt Z \alpha_0(t) \psi(t) e^{\gamma(t) - \gamma(T_e)} \right\|^2. \tag{4.46}$$

If we first compute the exponential term in eq.4.46, we find that

$$\gamma(t) = \left(\frac{1}{2} - i \frac{\Delta}{\kappa} \right) \log \frac{\int_0^t dt' \|\psi(t')\|^2}{\lim_{t \to 0} \int_0^t dt' \|\psi(t')\|^2}. \tag{4.47}$$

By calculating the difference between the two exponential terms $\gamma(t) - \gamma(T_e)$, we get rid of the divergent point, and we find:

$$\langle \hat{n}(T_e) \rangle = \int_0^{T_e} dt \|\psi(t)\|^2. \tag{4.48}$$

Since we considered the experimental time $T_e = 2T_\psi$, $\psi(t)$ is normalised in the interval $[0, T_e]$, and thus:

$$\langle \hat{n}(T_e) \rangle = 1. \tag{4.49}$$

Therefore, the photon is perfectly stored.

In the same way, using eq.4.24 and eq.4.47, we find the time evolution of the phonon operator $\hat{b}(t)$ in the adiabatic regime. This will be useful later for the study of the non-adiabatic regime. Using eq.4.24 with the optimal shape $\alpha_0(t)$, eq.4.41, yields:

$$\hat{b}(t) = \left[\int_0^t dt' \|\psi(t)\|^2 \right]^{\frac{1}{2} + i\frac{\Delta}{\kappa}}, \tag{4.50}$$

from which we also recover the result for $\langle \hat{n}(t) \rangle = \langle \hat{b}^\dagger(t) \hat{b}(t) \rangle$ found in eq.4.48.

In fig.4.2 we plot the numerically obtained $\langle \hat{n}_b \rangle$ as a function of time. As it is possible to see for $t \geq T_\psi$ the storage efficiency η, is maximised. We considered a single photon with $\psi(t) = \left(\frac{2}{\sigma\pi}\right)^{\frac{1}{2}} sin\left(\frac{t}{\sigma}\right)$, $\sigma = 100[a.u]$, $T_\psi = \sigma\pi$ and $T_e = 2T_\psi$. A cavity loss rate $\kappa = 1[a.u]$ has been assumed. σ and κ are in arbitrary units of time and frequency respectively, such that $\kappa\sigma$ is dimensionless. The condition of adiabaticity $\kappa\sigma \gg 1$ is thus fulfilled.

In fig.4.3 we compare the analytical result, eq.4.24, with the efficiency computed numerically, by plotting the absolute error between them.

The residual error in fig.4.3 is proportional to $(\kappa\sigma)^{-2}$. We later on derive an analytical proof of this fact.

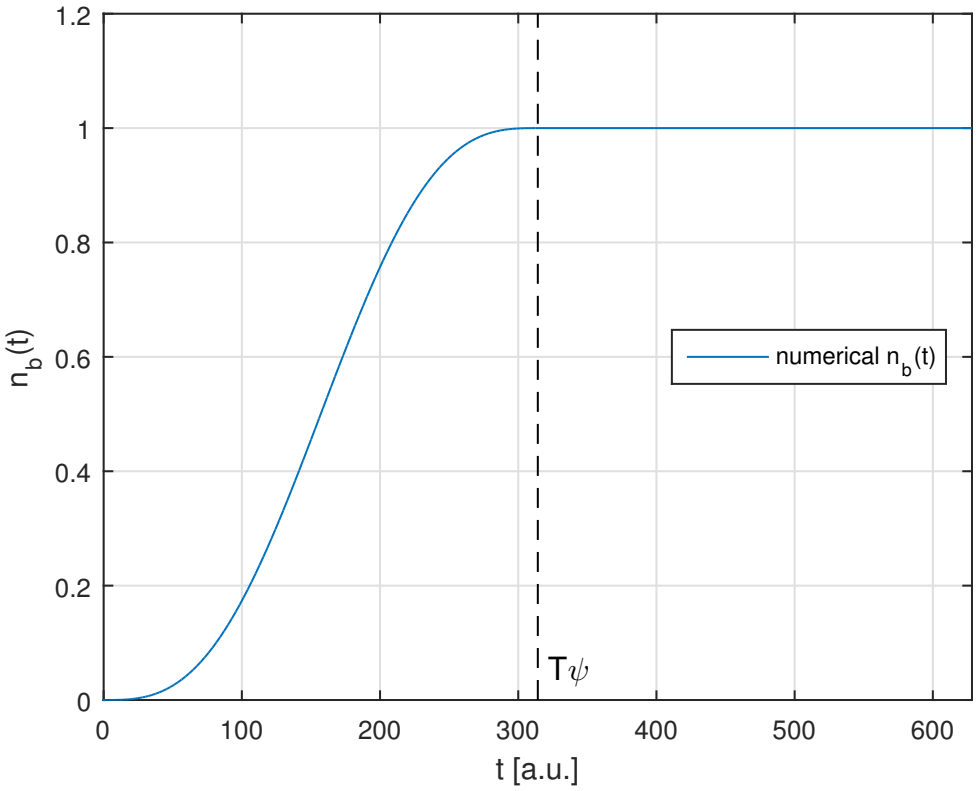

Figure 4.2: Number of phonons in the membrane with the optimal control pulse $\alpha_0(t)$ in the adiabatic regime. $\psi(t) = \left(\frac{2}{\sigma\pi}\right)^{\frac{1}{2}} sin\left(\frac{t}{\sigma}\right)$, $\sigma = 100[a.u]$, $T_\psi = \sigma\pi$, $T_e = 2T_\psi$ $\kappa\sigma = 100$, $\Delta = 0$.

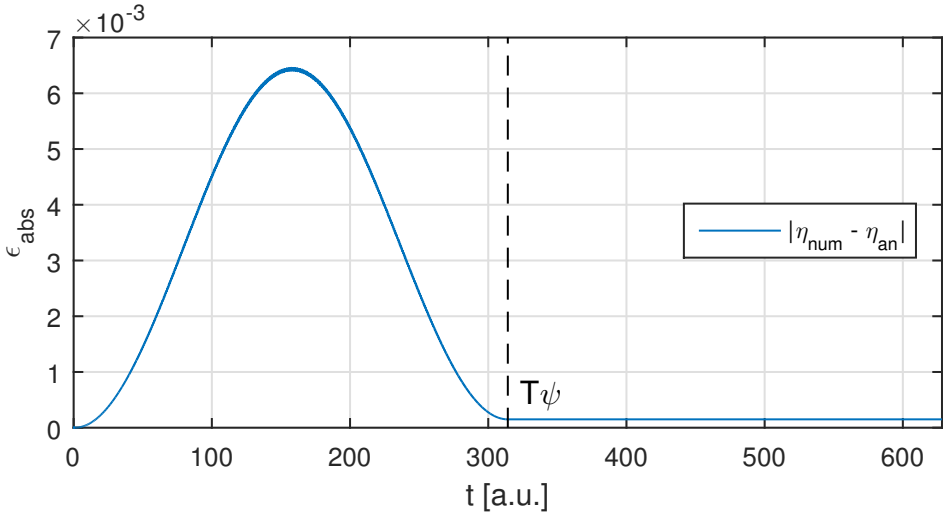

Figure 4.3: Absolute error ϵ_{abs} between numerical and analytical computations of the storage efficiency. $\psi(t) = \left(\frac{2}{\sigma\pi}\right)^{\frac{1}{2}} sin\left(\frac{t}{\sigma}\right)$, $\sigma = 100[a.u]$, $T_\psi = \sigma\pi$, $T_e = 2T_\psi$ $\kappa\sigma = 100$, $\Delta = 0$.

4.3 Non adiabatic regime

In this section we investigate the non adiabatic regime of our quantum memory. We first explore numerically its main features, and then develop a mathematical method that allows us to find analytical results. Our framework is not restricted to our specific problem, and can be used to study the non adiabatic regime of linear differential equations in general. We use a perturbative expansion for pushing the adiabatic limit to higher orders.

In the following, we assume $\alpha(t) = \alpha_0(t)$, the optimal pulse shape in the adiabatic regime, and study how the efficiency decreases with the parameter characterising the adiabaticity of our system, $\kappa\sigma$.

4.3.1 Numerical exploration of the non adiabatic regime

As we have seen above, when the adiabatic condition $\kappa\sigma \ll 1$ is fulfilled, we can always reach a unitary efficiency for the photon storage. This is done by properly adjusting the classical driving field according to eq.4.41.

Using the numerical approach of section 4.1, we study the system with a Gaussian-shaped single photon and the optimal driving pulse $\alpha_0(t)$. In this case, we identify the time-scale of the quantum pulse σ with the variance of the Gaussian distribution. By decreasing the width for a fixed value of κ, we enter the non-adiabatic regime, and investigate the decrease in efficiency.

In fig.4.4 we see how, even with the optimal pulse, the storage efficiency decreases with $\kappa\sigma$. The pulse $\alpha_0()$ in eq.4.41 is no longer optimal in the non adiabatic regime. It is also noticeable that, as we approach the adiabatic regime, the better efficiency comes at the cost of longer times in the storage process (this is, in the end, what *doing things adiabatically* means).

Investigating the efficiency achieved with different shapes $\psi(t)$, we find the results plotted in fig.4.5. We consider the four possibilities:

$$\psi_1(t) = \frac{e^{-\frac{t^2}{4\sigma^2}}}{(\sigma^2 2\pi)^{\frac{1}{4}}}, \tag{4.51}$$

$$\psi_2(t) = \frac{\sqrt{2t}}{\sigma} \qquad 0 \leq t \leq \sigma, \tag{4.52}$$

$$\psi_3(t) = sin\left(\frac{t}{\sigma}\right)\left(\frac{2}{\sigma\pi}\right)^{\frac{1}{2}} \qquad 0 \leq t \leq \pi\sigma, \tag{4.53}$$

$$\psi_4(t) = \frac{e^{\frac{t}{\sigma}}}{\sqrt{\sigma\frac{e^2-1}{2}}} \qquad 0 \leq t \leq \sigma. \tag{4.54}$$

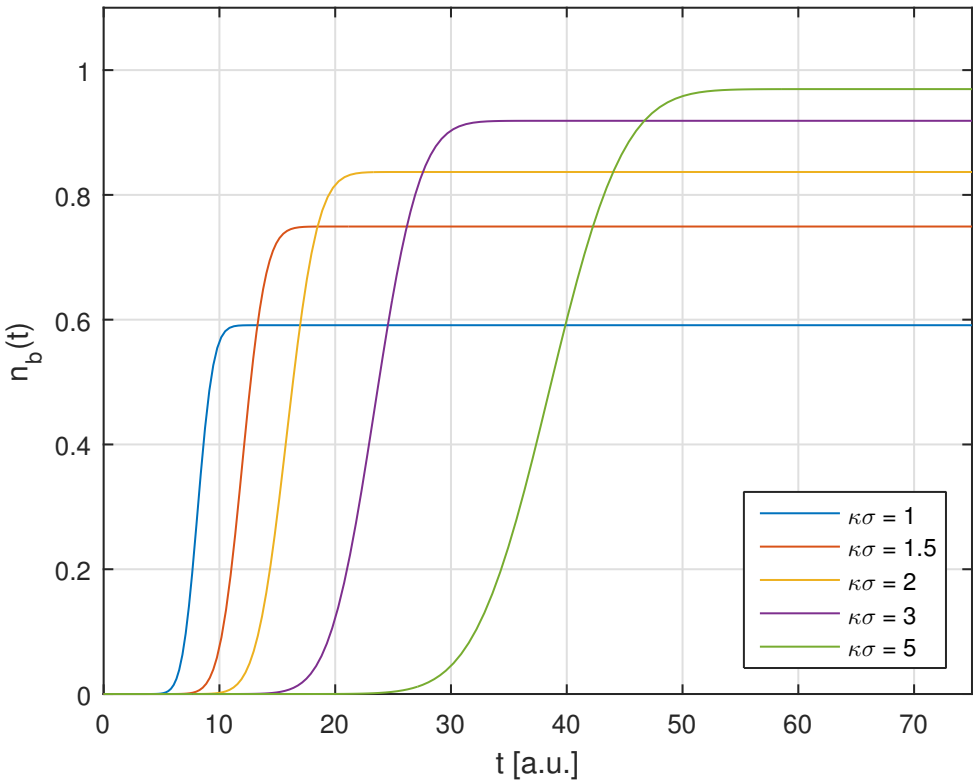

Figure 4.4: Number of phonons in the membrane as a function of time for a Gaussian single photon, $\psi(t) = \left(\frac{2}{\sigma\pi}\right)^{\frac{1}{2}} sin\left(\frac{t}{\sigma}\right)$, for different values of $\kappa\sigma$.

We see that the single photon shape is a critical factor for the storage efficiency. Some shapes behave better than others, and we want to understand why. To do so, we expand the efficiency curves in powers of $\frac{1}{\kappa\sigma}$:

$$\eta_i = 1 - \sum \frac{c_n^{(i)}}{(\kappa\sigma)^n}, \tag{4.55}$$

where the index i refers to the shape ψ_i considered. For the different shapes, and by choosing $\alpha_0(t)$ according to eq.4.41, the first non-zero terms in the series eq.4.55 are different. Thus, the efficiency of some shapes scale proportionally to $(\kappa\sigma)^{-1}$, while to $(\kappa\sigma)^{-2}$ for some others. The adiabaticity condition of the system is fulfilled at different values of $\kappa\sigma$

using different shapes.

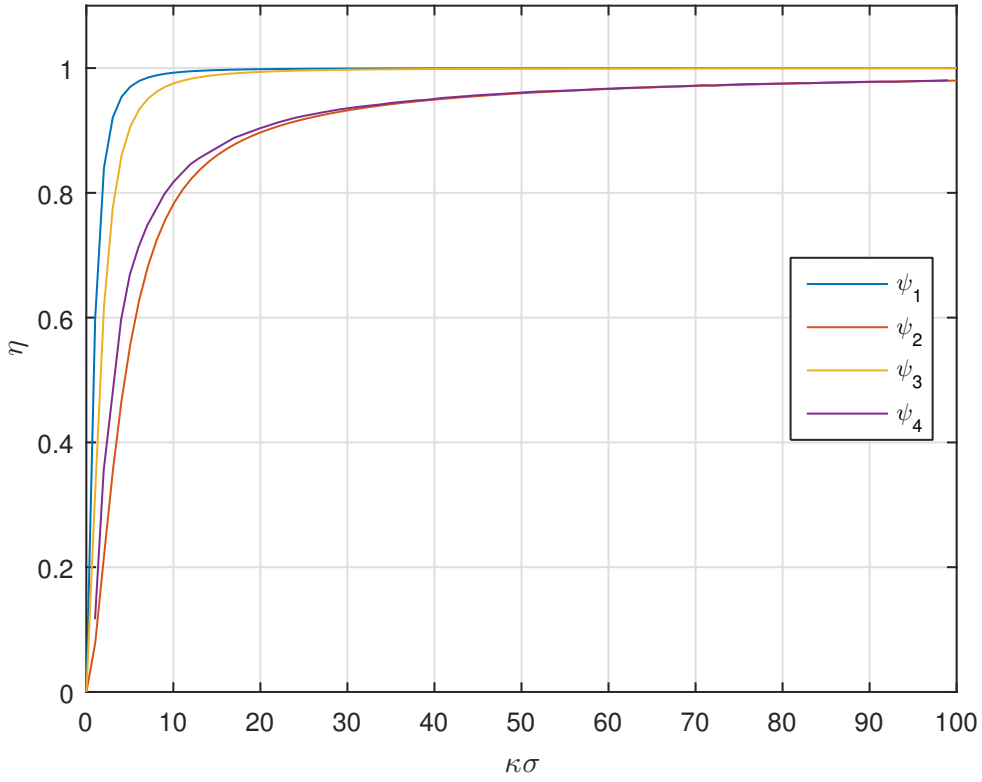

Figure 4.5: Storage efficiency as a function of the parameter $\kappa\sigma$ for various single photon shapes. In particular, $\psi_{1,2,3,4}$ are given in eqs.4.51-4.54.

By plotting $1-\eta_i$ and the dashed lines representing $(\kappa\sigma)^{-1}$ and $(\kappa\sigma)^{-2}$, we can qualitatively conclude that $\psi_2(t)$ and $\psi_4(t)$, eq.4.52 and eq.4.54 respectively, only get a first order contribution:

$$\eta_{2,4} \approx 1 - \frac{c_1^{(2,4)}}{\kappa\sigma}. \tag{4.56}$$

On the other hand, for $\psi_1(t)$ and $\psi_3(t)$, eq.4.51 and eq.4.53 respectively, we get a second order contribution, whereas the first order is negligible:

$$\eta_{1,3} \approx 1 - \frac{c_2^{(1,3)}}{(\kappa\sigma)^2}. \tag{4.57}$$

Thus, for the Gaussian and sinusoidal single photons, the non-adiabatic contributions become important at lower values of $\kappa\sigma$, and the driving field $\alpha_0(t)$ is optimal for a wider range of the adiabatic parameter.

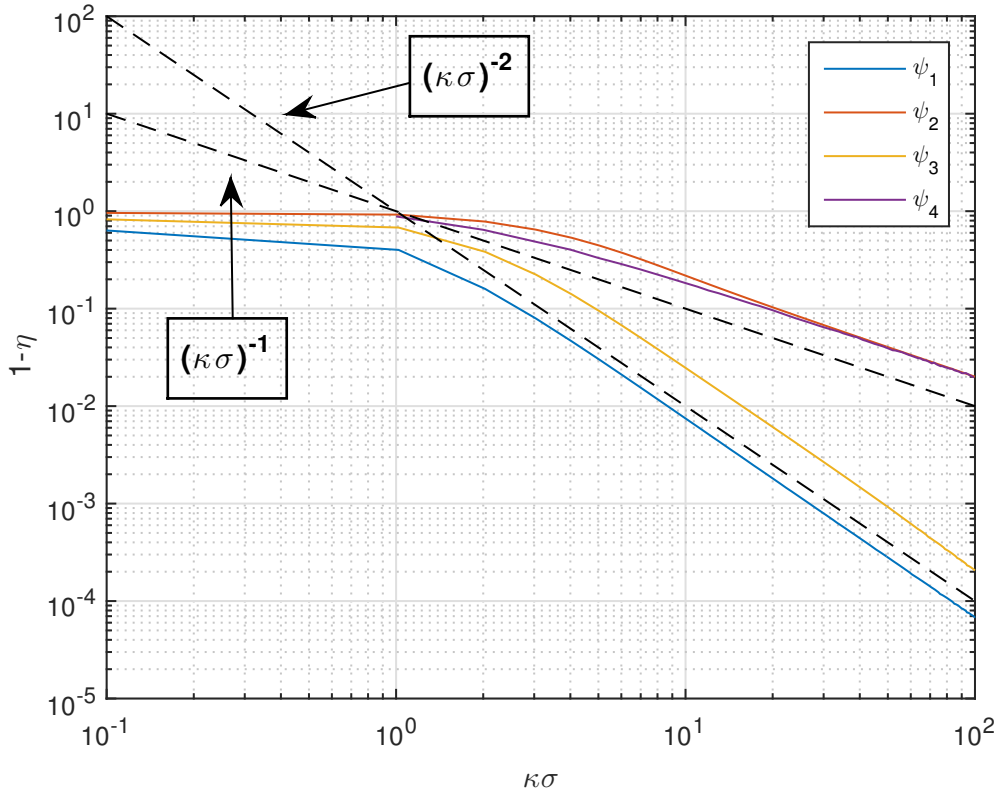

Figure 4.6: $1 - \eta_i$ (solid lines) in a logarithmic scale for the different shapes $\psi_{1,2,3,4}$, eqs.4.51-4.54. The dashed lines, $(\kappa\sigma)^{-1}$ and $(\kappa\sigma)^{-2}$, are used to qualitatively understand the behaviour of the efficiency.

Another feature that we can extract from our numerical simulations is the role of the detuning Δ. For any of the single photon shapes with a first order correction in their efficiencies, $\psi_2(t)$ and $\psi_4(t)$, the detuning does not change the efficiency. On the other hand, for $\psi_1(t)$ and $\psi_3(t)$, which only have a second order correction, the efficiency changes for different values of the detuning Δ. Notice that, by changing the detuning Δ, the blue sideband may contribute. In particular, for $\Delta \gg \kappa$, our results need to be generalised by considering the full Hamiltonian in eq.2.55.

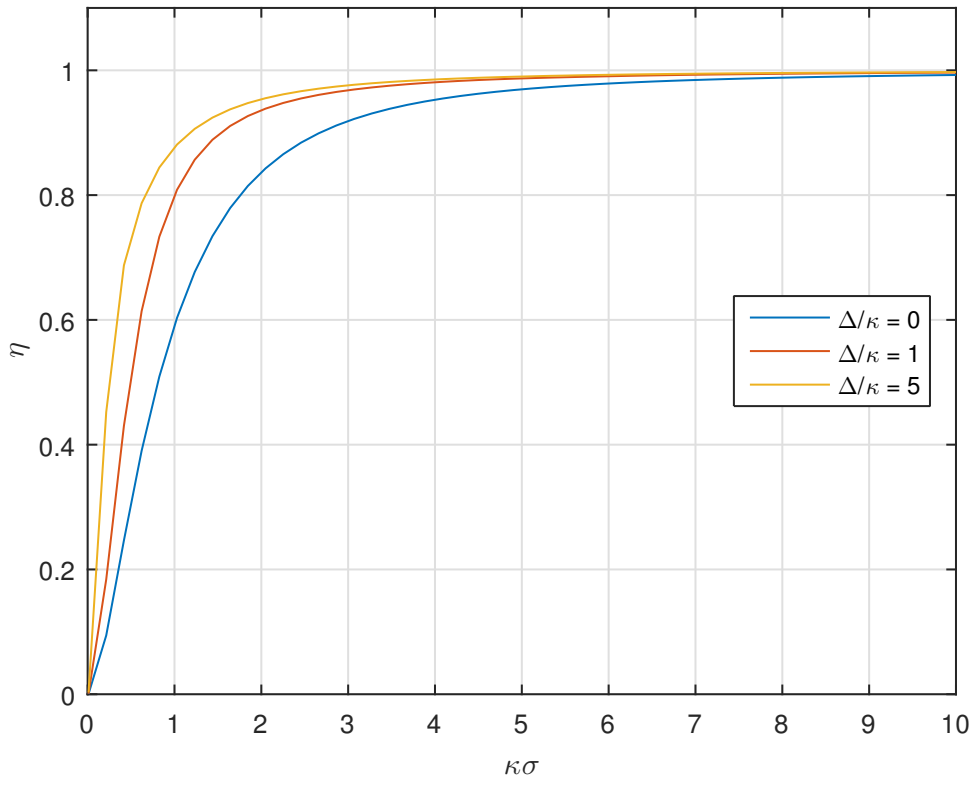

Figure 4.7: Storage efficiency of a single photon with a Gaussian shape, for different values of detuning.

In fig4.7 we plot the storage efficiency of a single photon with a Gaussian shape, eq.4.51, for different values of the parameter $\frac{\Delta}{\kappa}$. We can see how, increasing this value, the adiabaticity of the system is more solid.

4.3.2 Pushing the adiabatic limit

In physical systems described by differential equations, it may be difficult or even impossible to find analytic solutions, with only numerical results available. In some cases, however, such numerical results are not sufficient to understand the physics of the system. An analytic description is therefore needed in order to exploit some of its properties, and approximations in the equations of motion have to be made. Under certain circumstances, as we have seen trough all this work so far, it is very useful to study systems by performing an adiabatic elimination. Nevertheless, this approximation is only valid within a certain range of the parameters describing the system. Since the interesting features usually appear outside this narrow regime, in the following we introduce a framework that allows us to extend that range up to an arbitrary precision.

In other words, we present a mathematical method that allows us to study physical systems outside the adiabatic regime.

Let us consider a general function $f(t)$ in a neighbourhood of a given point $t_0 \in \Re$, and let it be infinitely differentiable and continuous in a given vicinity of t_0, say, $\Delta t = (t_0 - \Delta t_L, t_0 + \Delta t_R)$. Assume that such a function is not given, but is the solution of a system of two coupled first order ordinary differential equations that can be written, in a general form, as:

$$\frac{df(t)}{dt} = a(t) f(t) + b(t) q(t), \tag{4.58}$$

$$\frac{dq(t)}{dt} = c(t) q(t) + d(t) f(t), \tag{4.59}$$

where $a(t)$, $b(t)$, $c(t)$ and $d(t)$ are also assumed to be infinitely differentiable and continuous in the considered interval Δt.

Assume that, for the functions given $a(t)$, $b(t)$, $c(t)$ and $d(t)$, eq.4.58 can be adiabatically eliminated:

$$\left\| \frac{df(t)}{dt} \right\| \approx 0, \forall t \in \Delta t. \tag{4.60}$$

Thus we can express the function $f(t)$ as an adiabatic solution to our differential equation eq.4.58:

$$f(t) \approx f_0(t) = -\frac{b(t)}{a(t)} q(t), \tag{4.61}$$

which will be valid in the specified regime identified by the functions $a(t)$ and $b(t)$. At this point it is always possible to find an approximate solution $q_0(t)$ for $q(t)$ by solving eq.4.59 with eq.4.61. An analytical solution of the system of differential equations is therefore available in such regime.

Assume now that the given functions $a(t)$ and $b(t)$ do not satisfy condition eq.4.60. This implies that the error between the exact solution and the approximated in eq.4.61 is not negligible. In order to approximate the solution in this new regime, let us express $f(t)$ as a perturbative expansion around the adiabatic point, so that, to first order:

$$f(t) \approx f_0(t) + f_1(t), \tag{4.62}$$

where $f_0(t)$ is the solution found by adiabatically eliminating eq.4.58 above.

Recalling now the differential equation for $f(t)$, eq.4.58, we can plug eq.4.62 into it to get:

$$\frac{df_0(t)}{dt} + \frac{df_1(t)}{dt} = a(t) f(t) + b(t) q(t). \tag{4.63}$$

Let us assume that, in this new regime, the functions $a(t)$, $b(t)$, $c(t)$ and $d(t)$ are such that we can adiabatically eliminate the first correction $f_1(t)$ in eq.4.63. Using eq.4.61, this condition is fulfilled if

$$\left\| \frac{d}{dt}\left\{ \frac{1}{a(t)} \frac{d}{dt}\left\{ \frac{b(t)}{a(t)} q(t) \right\} \right\} \right\| \approx 0. \tag{4.64}$$

By adiabatically eliminating $f_1(t)$ in eq4.63 the perturbative solution can be expressed as:

$$f(t) \approx \underbrace{-\frac{b(t)}{a(t)} q(t)}_{f_0(t)} + \underbrace{\frac{1}{a(t)} \frac{df_0(t)}{dt}}_{f_1(t)}, \tag{4.65}$$

where we can now identify the terms $f_0(t)$ and $f_1(t)$ by comparison with eq.4.61 and eq.4.62. By collecting the leading terms in the expansion, we can find the correction $q_1(t)$ by plugging eq.4.65 into eq.4.59.

If $\| \frac{df_1(t)}{dt} \| \gtrsim 0$, we can consider a second order expansion. In the same fashion described above, we have:

$$\frac{df_0(t)}{dt} + \frac{df_1(t)}{dt} + \frac{df_2(t)}{dt} = a(t) f(t) + b(t) q(t). \tag{4.66}$$

Following the same procedure, assume that in a regime further away the adiabatic point the second order correction can be adiabatically eliminated, yielding the solution:

$$f(t) = \underbrace{-\frac{b(t)}{a(t)} q(t)}_{f_0(t)} + \underbrace{\frac{1}{a(t)} \frac{df_0(t)}{dt}}_{f_1(t)} + \underbrace{\frac{1}{a(t)} \frac{df_1(t)}{dt}}_{f_2(t)}, \tag{4.67}$$

which is valid if

$$\left\| \frac{d}{dt}\left\{ \frac{1}{a(t)} \frac{d}{dt}\left\{ \frac{1}{a(t)} \frac{d}{dt}\left\{ \frac{b(t)}{a(t)} q(t) \right\} \right\} \right\} \right\| \approx 0. \tag{4.68}$$

By iterating this process, it can be seen that the solution to the differential equation eq.4.58 can be expressed as an expansion of the form

$$f(t) \approx \sum_{n=0}^{N} f_n(t), \tag{4.69}$$

where each term in the sum is given by the recursive relation:

$$f_n(t) = \frac{1}{a(t)} \frac{df_{n-1}(t)}{dt}. \tag{4.70}$$

The initial term, $f_0(t)$, is the one obtained in eq.4.61. The n-th order solution is a good approximation to the exact solution $f(t)$ if:

$$\left\| D^{n+1} b(t) q(t) \right\| \approx 0. \tag{4.71}$$

Here we defined the differential operator $D = \frac{d}{dt}\frac{1}{a(t)}$. The derivative in D applies to all functions to its right, as can be seen in eq.4.64 and eq.4.68.

We developed a theory that allows us to perform an expansion of the function $f(t)$ and $q(t)$. In the following, we include explicitly the series for $q(t)$:

$$q(t) \approx \sum_{n=0}^{N} q_n(t), \tag{4.72}$$

and determine the coefficients $f_n(t)$ and $q_n(t)$ to leading order. In fact, by looking at eq.4.61, it is clear that $f_0(t)$ is not accessible, as $q(t)$ is unknown.

By plugging eq. 4.72 into eq.4.69, with the recursive relation eq.4.70 we can rewrite the perturbative solution to $f(t)$ as:

$$f(t) = \underbrace{-\frac{b(t)}{a(t)} q_0(t)}_{(0)} \underbrace{-\frac{b(t)}{a(t)} q_1(t)}_{(1)} \underbrace{-\frac{b(t)}{a(t)} q_0(t)}_{(2)} + \ldots +$$

$$-\frac{1}{a(t)}\frac{d}{dt}\left[\underbrace{-\frac{b(t)}{a(t)} q_0(t)}_{(1)} \underbrace{-\frac{b(t)}{a(t)} q_1(t)}_{(2)} \underbrace{-\frac{b(t)}{a(t)} q_2(t)}_{(3)} + \ldots \right] +$$

$$-\frac{1}{a(t)}\frac{d}{dt}\left[\frac{1}{a(t)}\frac{d}{dt}\left[\underbrace{-\frac{b(t)}{a(t)} q_0(t)}_{(2)} \underbrace{-\frac{b(t)}{a(t)} q_1(t)}_{(3)} \underbrace{-\frac{b(t)}{a(t)} q_2(t)}_{(4)} + \ldots \right] \right] + \ldots \tag{4.73}$$

By neglecting higher order terms and properly regrouping them, we define:

$$\tilde{f}_0(t) = -\frac{b(t)}{a(t)} q_0(t), \tag{4.74}$$

$$\tilde{f}_1(t) = -\frac{b(t)}{a(t)} q_1(t) - \frac{1}{a(t)} \frac{d}{dt} \frac{b(t)}{a(t)} q_0(t), \tag{4.75}$$

$$\tilde{f}_2(t) = -\frac{b(t)}{a(t)} q_2(t) - \frac{1}{a(t)} \frac{d}{dt} \frac{b(t)}{a(t)} q_1(t) - \frac{1}{a(t)} \frac{d}{dt} \left[\frac{1}{a(t)} \frac{d}{dt} \frac{b(t)}{a(t)} q_0(t) \right], \tag{4.76}$$

where now each of the terms $\tilde{f}_n$ only collects the n-th order correction of the exact solution. The solutions $\tilde{f}_n(t)$ follow the recursive relation:

$$\tilde{f}_n(t) = -\frac{b(t)}{a(t)} q_n(t) + \frac{1}{a(t)} \frac{d\tilde{f}_{n-1}(t)}{dt}. \tag{4.77}$$

With these new definitions, $f(t)$ can be finally rewritten:

$$f(t) \approx \sum_{n=0}^{N} \tilde{f}_n(t), \tag{4.78}$$

where now each of the $\tilde{f}_n(t)$ can be easily determined.

Plugging solution eq.4.78 into eq.4.59, we can solve for the n-th order contribution to the perturbation expansion in 4.72 as:

$$\frac{dq_n(t)}{dt} = c(t) q_n(t) + d(t) \tilde{f}_n(t). \tag{4.79}$$

For simplicity, consider $a(t)$ in eq.4.58 to be a constant $a(t) = a$. In this case, the solutions to the n-th order perturbation corrections are given by:

$$q_n(t) = e^{-\int_0^t dt' \left[c(t') - \frac{b(t')}{a} \right]} \left[q_n(0) - \frac{1}{a} \int_0^t dt' \sum_{j=1}^{n} \frac{d^j}{dt^j} \frac{b(t') q_{n-j}(t')}{a^j} e^{\int_0^{t'} dt'' \left[c(t'') - \frac{b(t'')}{a} \right]} \right], \tag{4.80}$$

$$\tilde{f}_n(t) = -\frac{b}{a} \sum_{j=0}^{n} \frac{d^j}{dt^j} \frac{q_{n-j}(t)}{a^j}. \tag{4.81}$$

These solutions are valid in a regime such that

$$\|a^n\| \gg \left\| \frac{d^n \tilde{f}_0(t)}{dt^n} \right\|. \tag{4.82}$$

With this results and equations 4.72 and 4.78, we can finally get an analytical solution to the system of coupled differential equations, eq.4.58 and eq.4.59, outside the adiabatic regime. These solutions can be tailored to approximate the real functions $f(t)$ and $q(t)$ to an arbitrary precision, as just as condition eq.4.82 is fulfilled.

4.3.3 Analytic solution in the non adiabatic regime

In our numerical analysis of the non adiabatic regime, we concluded that the efficiency of our memory can be expressed as a sum of various terms, eq.4.55, the first equal to 1 (the efficiency in the adiabatic regime is always maximum with the proper input large field), and the others decreasing while incrementing the parameter $\kappa\sigma$. These higher order terms, $c_n^{(i)}$ (where n is the perturbation order and i the index in ψ_i), only depend on the shape of the input field. In fact, by looking at eq.4.56 and eq.4.57, we deduce that the photon shape is the only free variable. In this section, using the previously derived mathematical method, we determine the contributions $c_n^{(i)}$ for the shapes $\psi(t)$ and the control field $\alpha_0(t)$.

It is helpful to slightly modify our description of the system, and introduce the definition of a dimensionless time τ, such that $\sigma\tau = t$. As before, σ is the parameter used to describe the duration of the single photon pulses. With the dimensionless time τ we rewrite our system eq.4.2 and eq.4.3 of coupled differential equations in a more convenient way:

$$\dot{\hat{b}}(\tau) = -ig\sigma\alpha(\tau)\,\hat{a}(\tau), \tag{4.83}$$

$$\dot{\hat{a}}(\tau) = -\kappa\sigma\left(\frac{1}{2} + i\frac{\Delta}{\kappa}\right)\hat{a}(\tau) - ig\sigma\alpha^*(\tau)\,\hat{b}(\tau) + \sigma\sqrt{\kappa}\hat{a}_{in}(\tau). \tag{4.84}$$

By comparison to eqs.4.58 and 4.59, we deduce that the adiabatic condition derived in section 4.3.2, eq.4.82, reads:

$$\|(\kappa\sigma)^n\| \gg \left\|\frac{1}{\left(\frac{1}{2} + i\frac{\Delta}{\kappa}\right)^n}\right\| \left\|\frac{d^n\hat{a}_0(\tau)}{d\tau}\right\|, \tag{4.85}$$

where $\hat{a}_0(\tau)$ is the adiabatic solution found in eq.4.22.

According to the formalism derived above, we expand the operators $\hat{a}(\tau)$ and $\hat{b}(\tau)$ as:

$$\hat{a}(\tau) = \sum_{n=0}^{N} \hat{a}_n, \tag{4.86}$$

$$\hat{b}(\tau) = \sum_{n=0}^{N} \hat{b}_n. \tag{4.87}$$

The n-th order perturbative corrections to the field inside the cavity can be found with eq.4.77:

$$\hat{a}_n(\tau) = -\frac{ig\alpha^*(\tau)}{\kappa\left(\frac{1}{2} + i\frac{\Delta}{\kappa}\right)}\hat{b}_n(\tau) - \frac{1}{\kappa\sigma}\frac{\dot{\hat{a}}_{n-1}(\tau)}{\frac{1}{2} + i\frac{\Delta}{\kappa}}. \tag{4.88}$$

And, using and eq.4.79, the terms for the phonon dynamics are:

$$\dot{\hat{b}}_n(\tau) = -\frac{g^2\|\alpha(\tau)\|^2}{\kappa\left(\frac{1}{2} + i\frac{\Delta}{\kappa}\right)}\hat{b}_n(\tau) + \frac{1}{\kappa\sigma}\frac{ig\alpha(\tau)}{\frac{1}{2} + i\frac{\Delta}{\kappa}}\dot{\hat{a}}_{n-1}(\tau). \tag{4.89}$$

Here, the zeroth order contributions are given in eq.4.22 and eq.4.50, and completely determine all higher order corrections.

By formally integrating eq.4.89, we find the solution for the nth order correction term to the non adiabatic creation of phonons operator to be, for a general coherent pulse $\alpha(\tau)$:

$$\hat{b}_n(\tau) = \frac{ig}{\kappa\sigma\left(\frac{1}{2}+i\frac{\Delta}{\kappa}\right)}\int_0^\tau d\tau'\alpha\left(\tau'\right)\dot{\hat{a}}_{n-1}\left(\tau'\right)e^{\gamma(\tau')-\gamma(\tau)}. \tag{4.90}$$

Here, $\gamma(\tau)$ is the function defined in the adiabatic regime, eq.4.25. Substituting $\gamma(\tau)$ in eq.4.90 and considering the optimal coherent pulse $\alpha_0(t)$ derived for the adiabatic regime, eq.4.41, we find the expression for $\hat{b}_n(\tau)$:

$$\hat{b}_n(\tau) = -\frac{1}{\kappa\sigma}\left[\int_0^\tau d\tau'\|\psi(\tau)\|^2\right]^{-\frac{1}{2}+i\frac{\Delta}{\kappa}}\int_0^\tau d\tau'\sqrt{\kappa}\psi^*\left(\tau'\right)\dot{\hat{a}}_{n-1}\left(\tau'\right). \tag{4.91}$$

Above, we described how to derive all terms of the adiabatic expansion for the operator $\hat{b}(\tau)$. To any required precision, we can cut the expansion eq.4.87 to the relevant order, after which the higher order corrections become negligible. In the following, we compare the numerical results found in section 4.3.1 to our theoretical approach, for the different single photon shapes described in eqs.4.51-4.54

From the qualitative results in eq.4.56 and eq.4.57, we can restrict ourselves to perturbation expansions up to first and second order, depending on the photon shape ψ_i.

4.3.4 First order correction

The zeroth order contribution for the optical field inside the cavity can be found from eq.4.50 to be:

$$a_0(\tau) = \frac{\psi(\tau)}{\sqrt{\kappa}}. \tag{4.92}$$

Correspondingly, the zeroth order contribution to the mechanics has been already found in eq.4.50. The first order correction to the non adiabatic dynamics for the operator $\hat{b}$ can be found using eq.4.92 and eq.4.91:

$$b_1(\tau) = -\frac{1}{\kappa\sigma}\left[\int_0^\tau d\tau'\|\psi(\tau)\|^2\right]^{-\frac{1}{2}+i\frac{\Delta}{\kappa}}\int_0^\tau d\tau'\psi^*\left(\tau'\right)\dot{\psi}\left(\tau'\right). \tag{4.93}$$

Taking the single photon shapes $\psi_i(\tau)$ to be real, this last expression can be easily integrated and yields:

$$b_1(\tau) = -\frac{1}{\kappa\sigma}\left[\int_0^\tau d\tau\|\psi\left(\tau'\right)\|^2\right]^{-\frac{1}{2}+i\frac{\Delta}{\kappa}}\frac{\psi^2(\tau)-\psi^2(0)}{2}. \tag{4.94}$$

Recalling that the photon must be normalised over the experimental time T_e in order to ensure that all its energy is transferred to the membrane, we can compute $\hat{b}_1(T_e)$:

$$b_1(T_e) = -\frac{1}{\kappa\sigma}\frac{\psi^2(T_e) - \psi^2(0)}{2}. \tag{4.95}$$

By comparison to eq.4.56, and computing the contribution of $\hat{b}_1$ to the efficiency of our memory $\eta = \langle \hat{b}^\dagger(T_e)\,\hat{b}(T_e)\rangle$, we can determine the constant $c_1^{(i)}$:

$$c_1^{(i)} = -\psi_i^2(T_e) + \psi_i^2(0). \tag{4.96}$$

The storage efficiency is $\eta = 1 + \frac{c_1^{(i)}}{\kappa\sigma}$, in the non adiabatic regime where only a first order correction is needed, as it is for ψ_2 and ψ_4 in eqs.4.52 and 4.54.

With this last result, eq.4.96, we can explain some of the features discovered during the numerical analysis of the system.

First, we can distinguish two types of input single photons, depending on them having a first order correction or not. The shapes $\psi_i(\tau)$ that are equal at the beginning and at the final times of the experiment (and, therefore, all symmetric pulses) will not have a first order contribution. On the other hand, shapes for which $\psi(T_e) \neq \psi(0)$ present this first order correction, as proven by shapes $\psi_2(\tau)$ and $\psi_4(\tau)$ in fig.4.6.

Second, those shapes with a first order correction do not show a dependence in the detuning Δ. This dependence is not only *presumably* negligible, but analytically nonexistent in the regime where no higher order corrections in $\kappa\sigma$ are needed.

Lastly, we can see how, as we already expected, $c_1^{(i)}$ is only a shape-dependent function, and independent of the pulse width σ.

In fig.4.8 we plot both the numerical simulation and the analytic solution for the storage efficiency of the single photon $\psi_4(t)$, eq.4.54. In fig.4.9 we show the same results for $\psi_2(t)$, eq.4.53. We can see that for both shapes our theory is in good agreement with the numerical computations nearby the adiabatic limit, $\kappa\sigma \gg 1$.

As we discussed above, the first order corrections of the shapes $\psi_1(t)$ and $\psi_3(t)$ are zero, with the leading term being quadrative in $\frac{1}{\kappa\sigma}$.

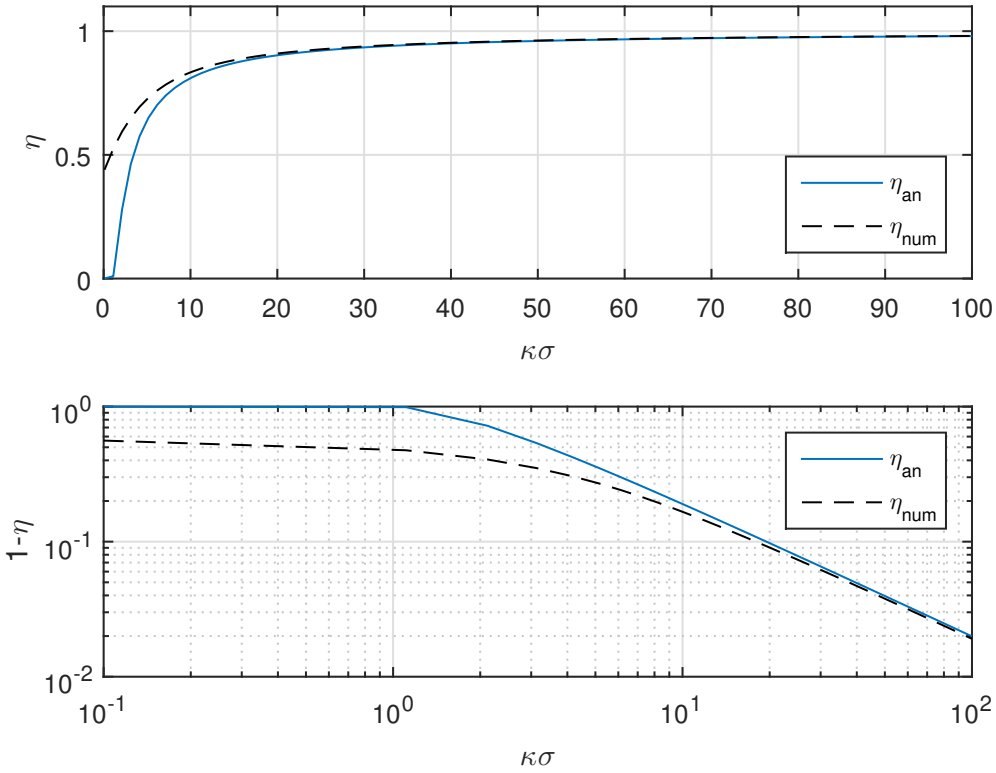

Figure 4.8: Comparison between the efficiency η obtained numerically (dashed) and by means of the analytic method developed (solid), for a single photon with shape $\psi_4(t)$, eq.4.54. η (top plot) and $1-\eta$ (bottom plot).

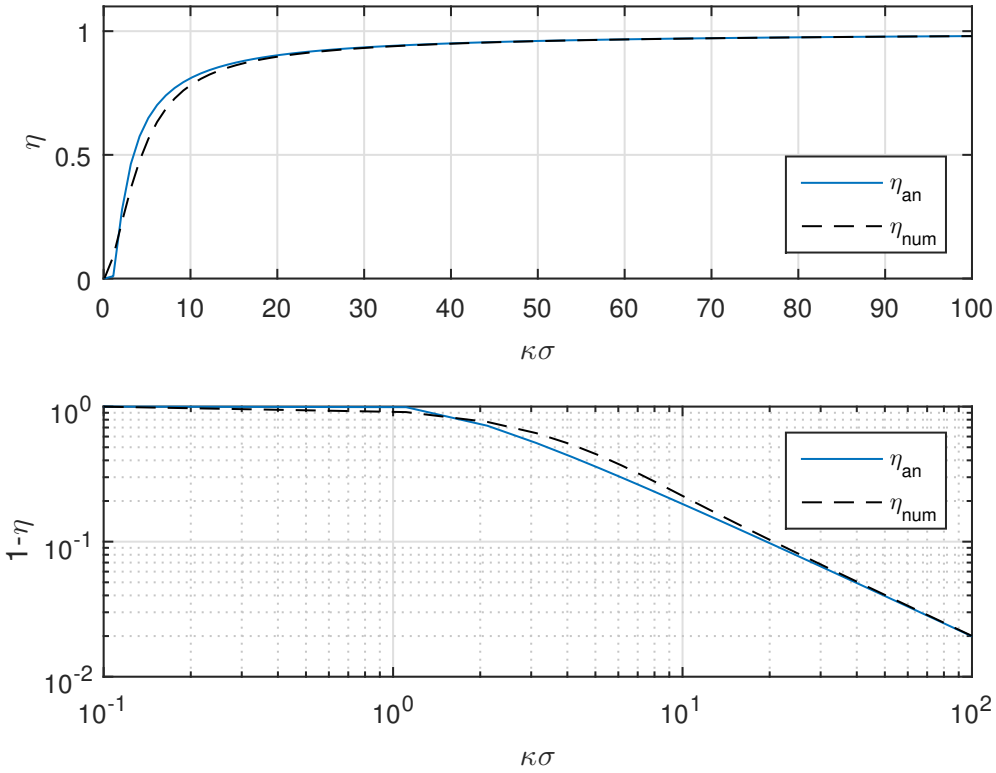

Figure 4.9: Comparison between the efficiency η obtained numerically (dashed) and by means of the analytic method developed (solid), for a single photon with shape $\psi_2(t)$, eq.4.52. η (top plot) and $1-\eta$ (bottom plot).

4.3.5 Second order correction

With the recursive relation for the non adiabatic corrections to the field inside the cavity, eq.4.88, and the results obtained above, eq.4.92 and eq.4.94, we can compute $\hat{a}_1(\tau)$:

$$a_1(\tau) = \frac{1}{\kappa\sigma}\frac{1}{\frac{1}{2}+i\frac{\Delta}{\kappa}}\frac{1}{\sqrt{\kappa}}\left[-\dot{\psi}(\tau)+\left(\frac{1}{2}-i\frac{\Delta}{\kappa}\right)\frac{\psi^3(\tau)}{2}\left[\int_0^\tau d\tau' \|\psi(\tau')\|^2\right]^{-1}\right]. \quad (4.97)$$

Here we assumed, for simplicity, that the experiment starts just before the single photon enters the cavity, such that $\psi(0)=0$. This is always fulfilled by all the photon shapes considered in our study, eqs.4.51-4.54.

Let us define $I(\tau)=\int_0^\tau d\tau' \|\psi(\tau')\|^2$. By plugging eq.4.97 into eq.4.91, we find the second order correction to the phononic dynamics:

$$b_2(\tau) = -\frac{I^{-\frac{1}{2}+i\frac{\Delta}{\kappa}}(\tau)}{(\kappa\sigma)^2}\int_0^\tau d\tau' \frac{\psi(\tau')}{\frac{1}{2}+i\frac{\Delta}{\kappa}}\left[\ddot{\psi}(\tau')+\right.$$

$$\left.-\left(\frac{1}{2}+i\frac{\Delta}{\kappa}\right)\frac{3\psi^2(\tau')\dot{\psi}(\tau')I^{-1}(\tau')-\psi^5(\tau')I^{-2}(\tau')}{2}\right]. \quad (4.98)$$

This yields the second constant $c_2^{(i)}$ in the expansion for η:

$$c_2^{(i)} = \frac{\|c_1^{(i)}\|^2}{2}+$$

$$-2\Re\left\{\int_0^{T_e} d\tau \frac{\psi_i(\tau)}{\frac{1}{2}+i\frac{\Delta}{\kappa}}\left[\ddot{\psi}_i(\tau)-\left(\frac{1}{2}+i\frac{\Delta}{\kappa}\right)\frac{3\psi_i^2(\tau)\dot{\psi}_i(\tau)I_i^{-1}(\tau)-\psi_i^5(\tau)I_i^{-2}(\tau)}{2}\right]\right\}. \quad (4.99)$$

With this, the storage efficiency is computed, to second order, as $\eta = 1+\frac{c_1^{(i)}}{\kappa\sigma}+\frac{c_2^{(i)}}{(\kappa\sigma)^2}$. Recall that, in our case, the second order corrections are needed when the first order $c_1^{(i)}$ is zero, and thus the first term in eq.4.99 will generally vanish.

According to previous discussions, we expected a leading second order contribution in the storage efficiency for the shapes $\psi_1(t)$ (eq.4.51) and $\psi_3(t)$ (eq.4.53). In fig.4.10 and fig.4.11 we plot the numerical and analytical results obtained for shapes $\psi_1(t)$ and $\psi_3(t)$, respectively. Our theory describes well the numerics, and confirms the quadratic behaviour of the efficiency η.

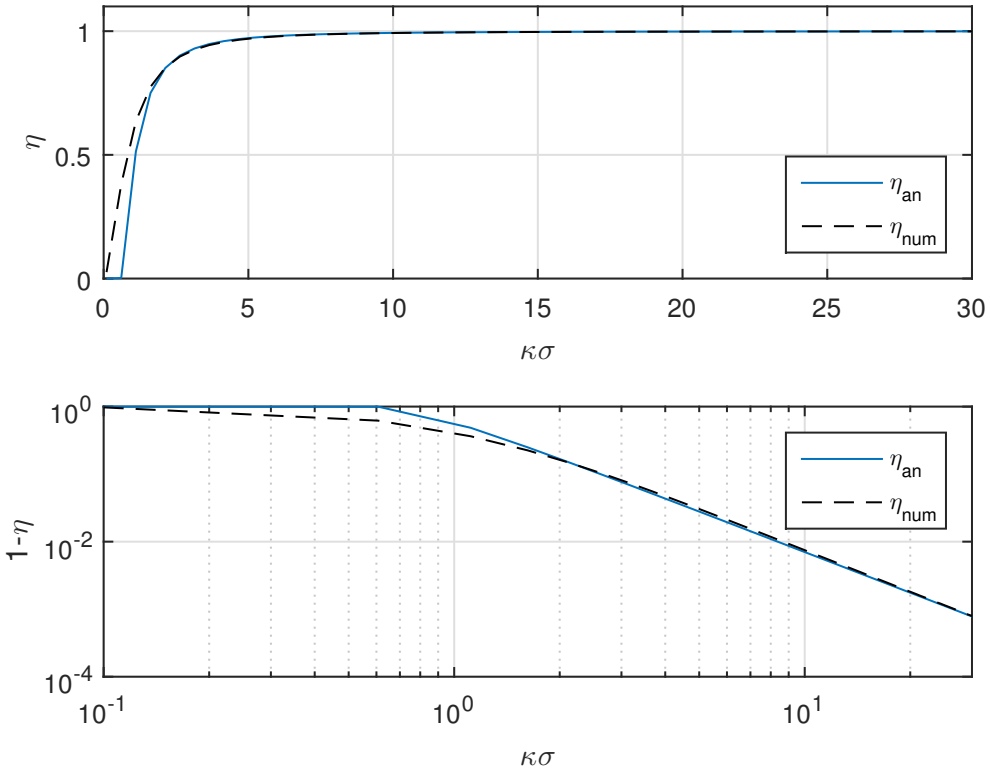

Figure 4.10: Comparison between the efficiency η obtained numerically (dashed) and by means of the analytic method developed (solid), for a single photon with shape $\psi_1(t)$, eq.4.51. η (top plot) and $1-\eta$ (bottom plot).

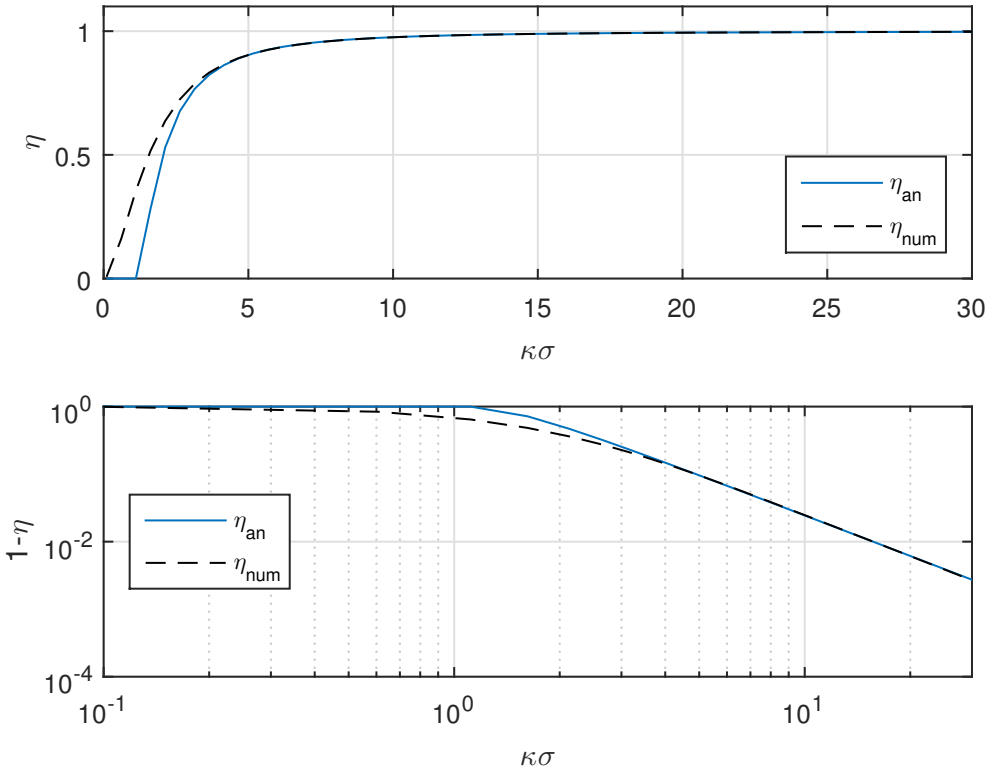

Figure 4.11: Comparison between the efficiency η obtained numerically (dashed) and by means of the analytic method developed (solid), for a single photon with shape $\psi_3(t)$, eq.4.53. η (top plot) and $1-\eta$ (bottom plot).

Differently from $c_1^{(i)}$, eq.4.96, in the expression for $c_2^{(i)}$, eq.4.99, the parameter $\frac{\Delta}{\kappa}$ does play a role. This was expected from the numerical analysis, as proven by fig.4.7. If we investigate the behaviour of the second order correction as a function of $\frac{\Delta}{\kappa}$, we find the results plotted in fig.4.12.

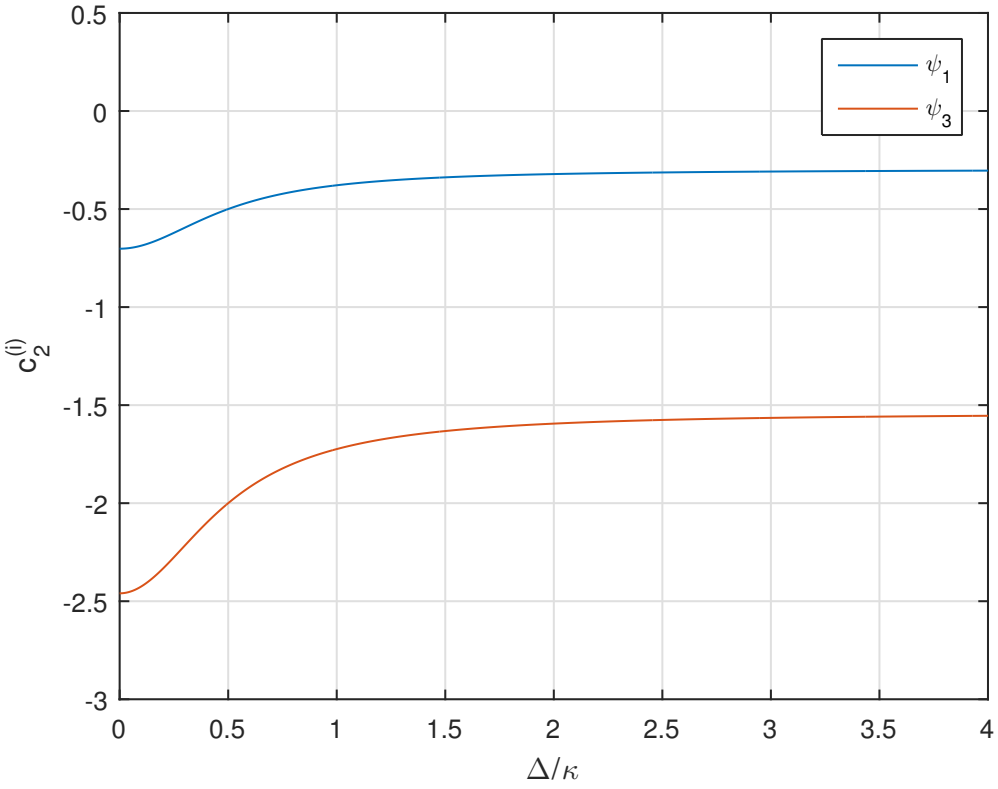

Figure 4.12: Value of $c_2^{(i)}$ as a function of $\frac{\Delta}{\kappa}$, for single photon shapes $\psi_1(t)$ and $\psi_3(t)$.

From fig.4.12 we conclude that to a higher detuning Δ is associated a lower absolute value of $c_2^{(i)}$. Moreover, $c_2^{(i)}$ is minimum for $\Delta = 0$, and asymptotically reaches a maximum as we increase the detuning. This is in complete accordance with the results found in the numerical investigation, fig.4.7. Recall, however, that both analytical and numerical results are derived without off resonant terms proportional to $\hat{a}\hat{b}$ and $\hat{a}^\dagger\hat{b}^\dagger$ in the interaction Hamiltonian. We expet this behaviour to be correct, as far as $\Delta \sim \kappa$.

It is interesting that the single photon shape $\psi_1(t)$ always presents a second order correction with a smaller absolute value than $\psi_3(t)$, $\|c_2^{(1)}\| < \|c_2^{(3)}\|$. Recalling that both

of them have $c_1^{(i)} = 0$, eq.4.96, we conclude that the Gaussian shape is more efficient for storage purposes. This is also in accordance with the numerical results plotted in fig.4.5. Finding the single photon shape that performs better is still an open question. However, with the results presented in this chapter, we an already exclude all shapes with a linear contribution.

Chapter 5

Conclusions and outlook

The photon storage efficiency is optimised in the adiabatic regime by mean of the coherent pulse $\alpha_0(t)$, eq.4.41. On the other hand, the non adiabatic regime can be analytically studied with the mathematical framework presented in chapter 4. Among all the considered possibilities, the Gaussian shape yields the best storage efficiency for short pulse photons. In particular, the process is optimised for a large detuning Δ.

In our work, we found a class of function $\psi(t)$ for which the efficiency scales quadratically with the adiabaticity parameter $\frac{1}{\kappa\sigma}$. As such, we pave the way for the pulse optimisation, excluding all the shapes for which the efficiency is linear in $\frac{1}{\kappa\sigma}$.

As an outlook, the single photon shape $\psi(t)$ could be further optimised by mean of a functional analysis of $c_2^{(i)}$, as well as for higher order contributions $c_n^{(i)}$ if required.

On the other hand, it would be interesting to derive analytical expressions for $\alpha_n(t)$. Here, $\alpha_n(t)$ is the shape of the control field that allows for optimal storage up to the n-th order, such that $c_n^{(i)} = 0$. This can be done by imposing that $\alpha_n(t)$ is such that does not allow the single photon escape. This is investigated in references [11] and [12] for atoms in a Λ configuration inside a cavity.

Finally, it would be interesting to extend our formalism outside the rotating wave approximation, as well as to investigate the effect of decay in the mechanical modes of the membrane.

Appendix A

Normalisation of the control function $\Upsilon(T_e, t)$

In chapter 4 we defined the control function $\Upsilon(T_e, t)$, eq.4.30. To derive the expression for the optimal shape $\alpha_0(t)$, it is required that $\Upsilon(T_e, t)$ is normalised.

By squaring eq.4.30, we get:

$$\|\Upsilon(T_e, t)\|^2 = \|Z\|^2 \|\alpha(t)\|^2 e^{\|Z\|^2 \int_{T_e}^{t} dt' \|\alpha(t')\|^2}. \tag{A.1}$$

With the change of variable

$$y(T_e, t) = \|Z\|^2 \int_{T_e}^{t} dt' \|\alpha(t')\|^2, \tag{A.2}$$

$$\frac{\partial}{\partial t} y(T_e, t) = \|Z\|^2 \|\alpha(t)\|^2, \tag{A.3}$$

we rewrite eq.A.1 as:

$$\|\Upsilon(T_e, t)\|^2 = \frac{\partial}{\partial t} y(T_e, t)\, e^{y(T_e, t)}. \tag{A.4}$$

Integrating eq.A.4 over time we get:

$$\int_{-\infty}^{+\infty} dt \frac{\partial}{\partial t} y(T_e, t)\, e^{y(T_e, t)} = e^{y(T_e, +\infty)} - e^{y(T_e, -\infty)} \tag{A.5}$$

The parameter T_e defines the final time of the experiment. Therefore, in the interval $t \in (T_e, +\infty)$ the pulse vanishes, yielding $\int_{T_e}^{+\infty} dt \|\alpha(t)\|^2 = 0$. Thus:

$$e^{y(T_e, +\infty)} = 1 \tag{A.6}$$

In order to compute the second exponential, recall the definition of the pulse $\alpha(t)$, eq.3.21. For a large number of photons N, we have:

$$\lim_{N \to +\infty} e^{-\|Z\|^2 \int_{-\infty}^{T_e} dt' \|\alpha(t')\|^2} = 0 \tag{A.7}$$

Plugging eq.A.6 and eq.A.7 into eq.A.5 yields:

$$\int_{-\infty}^{+\infty} dt \| \Upsilon \left(T_e, t \right) \|^2 = 1, \tag{A.8}$$

from which we prove that the control function $\Upsilon \left(T_e, t \right)$ is normalised.

Bibliography

[1] DiVincenzo, David P. (2000-04-13). "The Physical Implementation of Quantum Computation". Fortschritte der Physik. 48: 771–783.

[2] H.Häffner, C.F.Roos, R.Blatt, Quantum computing with trapped ions (2008)

[3] G Wendin 2017 Rep. Prog. Phys. 80 106001

[4] C. W. Gardiner and M. J. Collett, Physical Review A 31, 3761 (1985)

[5] Schwabl, Franz (2008). Advanced Quantum Mechanics (4th ed.). Springer. p. 253. ISBN 978-3-540-85062-5.

[6] R. Paschotta, article on 'finesse' in the Encyclopedia of Laser Physics and Technology, https://www.rp-photonics.com/finesse.html, accessed on 2018-07-25

[7] Alexey V. Gorshkov, Axel André, Mikhail D. Lukin and Anders S. Sørensen, Physical Review A 76, 033804 (2007)

[8] The Mathworks, Inc. (2018). Ordinary Differential Equations: User's Guide (R2018a), https://www.mathworks.com/help/matlab/ref/ode45.html, accessed on 2018-08-01

[9] Dormand, J. R. and P. J. Prince, "A family of embedded Runge-Kutta formulae," J. Comp. Appl. Math., Vol. 6, 1980, pp. 19–26.

[10] Shampine, L. F. and M. W. Reichelt, "The MATLAB ODE Suite," SIAM Journal on Scientific Computing, Vol. 18, 1997, pp. 1–22.

[11] Jerome Dilley, Peter Nisbet-Jones, Bruce W. Shore, and Axel Kuhn, Physical Review A 85, 023834 (2012)

[12] Luigi Giannelli, Tom Schmit, Tommaso Calarco, Christiane P. Koch, Stephan Ritter and Giovanna Morigi, "Optimal storage of a single photon by a single intra-cavity atom" (2018)

[13] Barg, A., Tsaturyan, Y., Belhage, E., Nielsen, W. H. P., Moller, C. B., Schliesser, A. (2017). Measuring and imaging nanomechanical motion with laser light. Applied Physics B, 123(4), [138]. DOI: 10.1007/s00340-017- 6722-y

[14] Dan Browne, Sougato Bose, Florian Mintert, and M. S. Kim, From Quantum Optics to Quantum Technologies (2017)

[15] M. A. Nielsen and I. L. Chuang, Quantum Computation and Quantum Information. Cambridge University Press, Cambridge, 2000

[16] Y. Tsaturyan, A. Barg, E. S. Polzik and A. Schliesser (2017) Ultracoherent nanomechanical resonators via soft clamping and dissipation dilution. Nature Nanotechnology. DOI: 10.1038/NNANO.2017.101

[17] Yeghishe Tsaturyan, Andreas Barg, Anders Simonsen, Luis Guillermo Villanueva, Silvan Schmid, Albert Schliesser, and Eugene S. Polzik. Optics Express. DOI:10.1364/OE.22.006810

[18] Kelly J. et al. (2015) State preservation by repetitive error detection in a superconducting quantum circuit. Nature 519 66–9

[19] Barends R. et al. (2016) Digitized adiabatic quantum computing with a superconducting circuit. Nature 534 222–6

[20] Shor, Peter W. (1997), "Polynomial-Time Algorithms for Prime Factorization and Discrete Logarithms on a Quantum Computer", SIAM J. Comput., 26 (5): 1484–1509

[21] David Deutsch and Richard Jozsa (1992). "Rapid solutions of problems by quantum computation". Proceedings of the Royal Society of London A. 439: 553

[22] Gulde, S., Haffner, H., Riebe, M., Lancaster, G., Becher, C., Eschner, J., Schmidt-Kaler, F., Chuang, I. L., Blatt, R. (2003). Quantum information processing with trapped Ca+ ions. Proc. R. Soc. Lond. A 361, 1363–1374.

[23] Gulde, S., 2003. Experimental realization of quantum gates and the deutschjosza algorithm with trapped 40Ca+–ions. Ph.D. thesis, Universität Innsbruck.

[24] Langer, C., Ozeri, R., Jost, J. D., Chiaverini, J., Demarco, B., Ben-Kish, A., Blakestad, R. B., Britton, J., Hume, D. B., Itano, W. M., Leibfried, D., Reichle, R., Rosenband, T., Schaetz, T., Schmidt, P. O., Wineland, D. J. (2005). Long-lived qubit memory using atomic ions. Phys. Rev. Lett. 95, 060502.

[25] Bollinger, J. J., Heinzen, D. J., Itano, W. M., Gilbert, S. L., Wineland, D. J. (1991). A 303 MHz frequency standard based on trapped Be+ ions. IEEE Trans. Instr. Meas. 40, 126.